PENSOFT
SENCKENBERG world of biodiversity
Leibniz Association

Description of six new species of *Cyrtodactylus* Gray (Squamata: Gekkonidae) from northeastern India

Bitupan Boruah[1], Surya Narayanan[2], Neelavar Ananthram Aravind[2,3], Samuel Lalronunga[4], V. Deepak[5,6], Abhijit Das[1]

1 *Wildlife Institute of India, Chandrabani, Dehradun, Uttarakhand 248001, India*
2 *SM Sehgal Foundation Center for Biodiversity and Conservation, Ashoka Trust for Research in Ecology and the Environment (ATREE), Royal Enclave, Srirampura, Bangalore, Karnataka 560064, India*
3 *Yenepoya Research Centre, Yenepoya University, Derlakatte, Mangalore, India*
4 *Holy Child Society, Nalkata, Tripura 799263, India*
5 *Department of Life Sciences, The Natural History Museum, London SW7 5BD, UK*
6 *School of Natural and Environmental Sciences, Newcastle University, Newcastle upon Tyne NE1 7RU, UK*

https://zoobank.org/154CE236-EFA8-4411-834B-234A9B45A63F

Corresponding author: Abhijit Das (abhijit@wii.gov.in)

Academic editor Uwe Fritz | **Received** 4 April 2024 | **Accepted** 6 July 2024 | **Published** 29 July 2024

Citation: Boruah B, Narayanan S, Aravind NA, Lalronunga S, Deepak V, Das A (2024) Description of six new species of *Cyrtodactylus* Gray (Squamata: Gekkonidae) from northeastern India. Vertebrate Zoology 74 453–486. https://doi.org/10.3897/vz.74.e124752

Abstract

We describe six new species of *Cyrtodactylus* from the *khasiensis* group using morphological characteristics, supported by the molecular analyses based on the mitochondrial ND2 gene. We used four different molecular species delimitation analyses that recovered six distinct undescribed lineages distributed across four states in northeastern India. Our phylogenetic analyses using ML and Bayesian approaches recovered a clade where the recently described *C. arunachalensis* and *C. cayuensis* align together with our other samples from Arunachal Pradesh, north of Brahmaputra River. Based on these results and overlapping morphological characteristics we synonymize *C. arunachalensis* with *C. cayuensis.* We provide updated comparative morphological characters for species in the *khasiensis* group and where available these characters are tabulated for males and females separately. Including the six new species the *khasiensis* group now contains 35 species, of which 26 are endemic to India.

Keywords

Himalaya, Indo-Burma Biodiversity Hotspot, molecular phylogeny, Sauria, taxonomy

Introduction

The gekkonid genus *Cyrtodactylus* Gray, 1827 is the second most speciose lizard group comprising 359 formally described species distributed widely across South Asia to Melanesia (Grismer et al. 2022, 2021; Uetz et al. 2024). Recently, Grismer et al. (2021) grouped 310 species of the genus into 31 groups, of which six occur in India (Grismer et al. 2021, 2022). Among these six groups, the *tibetanus*, *lawderanus*, *peguensis*, *fasciolatus* and *khasiensis* groups are distributed in the Himalayan and the Indo-Burma regions while the *triedrus* group is restricted to peninsular India and Sri Lanka (Grismer et al. 2021, 2022). Out of the five species groups found in northeastern India, the *khasiensis* group diversified approximately 28 mya in the area south of Brahmaputra River with a single lin-

eage distributed north of the river in the Himalayan foothills (100–300 m elevation above mean sea level [a.s.l.]) (Agarwal et al. 2014; Mirza et al. 2021; Grismer et al. 2022). Prior to this study there were 21 species included in the *khasiensis* group in northeastern India.

The recent upsurge in taxonomic studies of the *khasiensis* group has resulted in the description of 24 new species of *Cyrtodactylus* during the last five years. Many of the new descriptions used morphological characters to corroborate the molecular analyses. While most of these studies, along with their morphological characteristics, used only ND2 mitochondrial gene others used this gene in conjugation with three nuclear genes to support the validity and phylogenetic position of the species described (Agarwal et al. 2018a, 2018b; Grismer et al. 2018, 2019; Purkayastha et al. 2020; Kamei and Mahony 2021; Liu and Rao 2021; Mahony and Kamei 2021; Mirza et al. 2021; Purkayastha et al. 2021, 2022; Bohra et al. 2022; Lalremsanga et al. 2022; Lalremsanga et al. 2023). The *khasiensis* group is diverse with 30 nominal species and three undescribed lineages (Grismer et al. 2021, 2022; Lalremsanga et al. 2023). Within the *khasiensis* group there are four sub-groups (referred as clades hereafter), the *khasiensis* clade (*C. bapme* Kamei & Mahony, 2021; *C. karsticola* Purkayastha et al., 2021; *C. agarwali* Purkayastha et al., 2021; *C. septentrionalis* Agarwal et al., 2021; *C. guwahatiensis* Purkayastha et al., 2020; *C. exercitus* Purkayastha et al., 2022; *C. urbanus* Purkayastha et al., 2018; *C. khasiensis* [Jerdon, 1870]; *C. ayeyarwadyensis* Bauer, 2003; *C. tripuraensis* Agarwal et al., 2018; *C. kazirangaensis* Agarwal et al., 2018); the *gansi* clade (*C. vairengtensis* Lalremsanga et al., 2023; *C. aaronbaueri* Purkayastha et al., 2021; *C. ngopensis* Bohra et al., 2022; *C. montanus* Agarwal et al., 2018; *C. lungleiensis* Lalremsanga et al., 2022; *C. siahaensis* Purkayastha et al., 2022; *C. bengkhuaiai* Purkayastha et al., 2021; *C. namtiram* Mahony & Kamei, 2021; *C. aunglini* Grismer et al., 2018; *C. chrysopylos* Bauer, 2003; *C. myaleiktaung* Grismer et al., 2018; *C. nagalandensis* Agarwal et al., 2018; *C. dianxiensis* Liu & Rao, 2021; *C. gansi* Bauer, 2003; *C. jaintiaensis* Agarwal et al., 2018; *C. brevidactylus* Bauer, 2002); the *mombergi* clade (*C. mombergi* Grismer et al., 2019); and the *arunachalensis* clade (*C. arunachalensis* Mirza et al., 2021). These clades were recognized by previous studies based on their monophyly (Grismer et al. 2018; Mahony and Kamei 2021; Che et al. 2022). Among these, the *arunachalensis* clade is distributed north of Brahmaputra River, while the remaining three groups are distributed south of the river.

Che et al. (2020) included samples of *C. cayuensis* Li, 2007 in their phylogeny, but included only representatives from the *khasiensis* and *gansi* clades. Although the position of *C. cayuensis* is recovered within the *khasiensis* group, its relationship within the group remains unclear (Che et al. 2020). Furthermore, molecular data are not available for two species from Burma, viz., *C. tamaiensis* (Smith, 1940) and *C. mandalayensis* Mahony, 2009. Hence, these species are currently not assigned to any of these aforementioned clades.

During our recent (2018–2022) surveys across northeastern India, we collected *Cyrtodactylus* spp. from 22 locations (Fig. 1; Table 1). We generated mitochondrial ND2

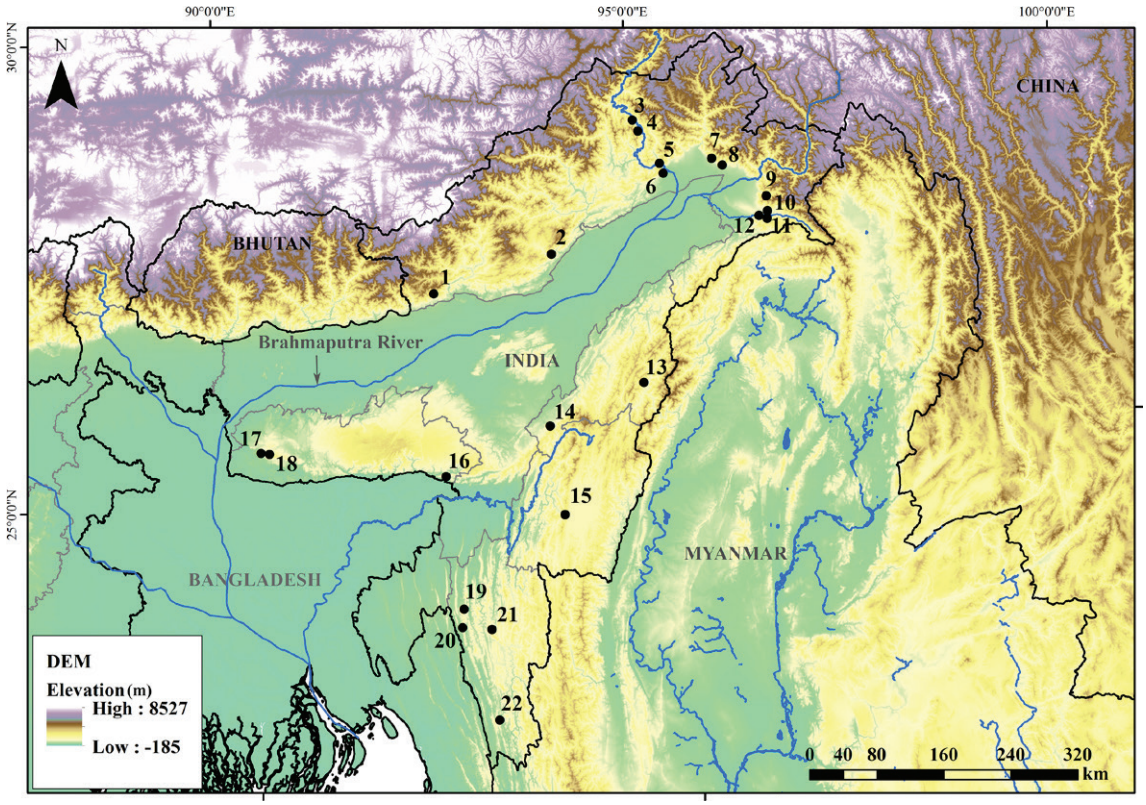

Figure 1. Map showing sampling localities for *Cyrtodactylus* in northeastern India. Numbers correspond to the locality names provided in Table 1.

Table 1. Gazetteer of sampling localities provided in Figure 1 and Figure 3B. Type localities are marked with asterisks.

No.	Localities marked in Figure 1			
	Locality name	**District**	**State**	**Geographical coordinates**
1	Sessni	West Kameng	Arunachal Pradesh	27.0509°N, 92.4150°E
2	Potin	Lower Subansiri	Arunachal Pradesh	27.3478°N, 93.8497°E
3	Ramsing, Mouling National Park	Upper Siang	Arunachal Pradesh	28.6563°N, 94.9795°E
4	Jengging	Upper Siang	Arunachal Pradesh	28.5340°N, 95.0305°E
5	Bodak*	East Siang	Arunachal Pradesh	28.1711°N, 95.2420°E
6	Balek	East Siang	Arunachal Pradesh	28.0624°N, 95.2721°E
7	Ezengo	Lower Dibang Valley	Arunachal Pradesh	28.1565°N, 95.8638°E
8	Diffo River	Lower Dibang Valley	Arunachal Pradesh	28.0732°N, 95.9784°E
9	Kamlang Tiger Reserve	Lohit	Arunachal Pradesh	27.6960°N, 96.4456°E
10	Hornbill, Namdapha Tiger Reserve	Changlang	Arunachal Pradesh	27.5381°N, 96.4403°E
11	Kamala Valley, Namdapha Tiger Reserve*	Changlang	Arunachal Pradesh	27.4608°N, 96.4260°E
12	Motijheel, Namdapha Tiger Reserve	Changlang	Arunachal Pradesh	27.4996°N, 96.3325°E
13	Forest colony, Kiphire forest division*	Kiphire	Nagaland	25.8994°N, 94.7694°E
14	Athibung*	Peren	Nagaland	25.5419°N, 93.6307°E
15	Lamdan Kabui*	Churachandpur	Manipur	24.5954°N, 93.7085°E
16	Norpuh Wildlife Sanctuary	East Jaintia Hills	Meghalaya	25.1099°N, 92.3715°E
17	Tura Peak	West Garo Hills	Meghalaya	25.5082°N, 90.2308°E
18	Daribokgre, Nokrek Biosphere Reserve	West Garo Hills	Meghalaya	25.4896°N, 90.3297°E
19	Teirei, Dampa Tiger Reserve	Mamit	Mizoram	23.6921°N, 92.4522°E
20	Phuldungsei, Dampa Tiger Reserve	Mamit	Mizoram	23.4992°N, 92.4162°E
21	Hmuifang	Aizawl	Mizoram	23.4535°N, 92.7523°E
22	Ngengpui Wildlife Sanctuary*	Lawngtlai	Mizoram	22.4906°N, 92.7575°E
No.	**Localities marked in Figure 3B**			
1	Seijosa	East Kameng	Arunachal Pradesh	26.9668°N, 93.0133°E
2	Dakte Hoj	Papum Pare	Arunachal Pradesh	27.3325°N, 93.8377°E
3	Potin	Lower Subansiri	Arunachal Pradesh	27.3478°N, 93.8497°E
4	Ramsing, Mouling National Park	Upper Siang	Arunachal Pradesh	28.6563°N, 94.9795°E
5	Jengging	Upper Siang	Arunachal Pradesh	28.5340°N, 95.0305°E
6	Bodak	East Siang	Arunachal Pradesh	28.1711°N, 95.2420°E
7	Balek	East Siang	Arunachal Pradesh	28.0624°N, 95.2721°E
8	Ezengo	Lower Dibang Valley	Arunachal Pradesh	28.1565°N, 95.8638°E
9	Diffo River	Lower Dibang Valley	Arunachal Pradesh	28.0732°N, 95.9784°E
10, 11	Hawa Pass	Lohit	Arunachal Pradesh	27.9166°N, 96.3323°E
12	Glaw lake, Kamlang Tiger Reserve	Lohit	Arunachal Pradesh	27.6960°N, 96.4456°E
13	Xizang	—	China	28.5421°N, 97.0483°E

gene and morphological characters for all these specimens. Our phylogenetic analyses and delimitation approaches suggested presence of six undescribed lineages within the *khasiensis* group that was congruent with our morphological findings. Herein we describe these six lineages as new species using morphological data. Furthermore, we clarify the systematic position of *C. cayuensis* within this group and discuss the validity of the recently described *C. arunachalensis* from Arunachal Pradesh, India.

Materials and methods

Field survey and specimen collection

Field surveys were carried out in Arunachal Pradesh, Mizoram, Meghalaya, Manipur and Nagaland during 2018–2022. Specimens were located visually at night using torches and photographed in life. Collected specimens were euthanized using Tricaine Methanesulfonate (MS222), fixed in 4% formalin and finally stored in 70% ethanol after being washed in water for 24 hours. Prior to fixation, liver tissue was collected and stored in molecular grade ethanol for DNA extraction. Specimens were deposited in the Wildlife Institute of India, Dehradun.

Molecular analysis

We extracted genomic DNA from liver tissue samples stored in absolute ethanol at –20°C, using the DNeasy (Qiagen) blood and tissue kit. We amplified the partial sequence (1038 base pairs) of the mitochondrial ND2 gene, for a total of 34 specimens using the following primers: MetF1 and H5934 (Macey et al. 1997). Resultant sequences ranged between 400 bp and 1000 bp. Polymerase

chain reaction (**PCR**) conditions were as described in Das et al. (2022). All sequences were deposited in GenBank with the registration numbers PQ009361–PQ009394 (see also Table S1).

Bidirectional sequences were manually checked using the CHROMAS v.2.6.6 software (http://technelysium.com.au/wp/chromas) and aligned using ClustalW (Thompson et al. 1994) with default prior settings implemented in MEGA v.7 (Kumar et al. 2016). We checked for unexpected stop codons by translating the sequence to amino acids in MEGA v.7 (Kumar et al. 2016). The new sequences generated in this study were aligned with 115 sequences of *Cyrtodactylus* from the *khasiensis* group deposited in GenBank and three other species from the *tibetanus* group that are used as outgroups and used as root for the phylogenetic analysis (see Table S1).

Maximum Likelihood (**ML**) analysis for the final dataset was carried out using the IQTREE (http://iqtree.cibiv.univie.ac.at) (Trifinopoulos et al. 2016). The best-fit models for the partition scheme suggested by the PartitionFinder v1.1.1 (Lanfear et al. 2017) were determined using the in-built Modelfinder (Kalyaanamoorthy et al. 2017) for the ML analysis. The best-fit models for the ML analysis are as follows, ND2 position1: TVM+F+G4, ND2 position2: TPM3u+F+G4, ND2 position3: TIM+F+I+G4. A Bayesian Inference (**BI**) analysis was carried out using MrBayes v.3.2 (Ronquist et al. 2012), with default prior settings. For this analysis, we used the best-fit models suggested by PartitionFinder for each partition as follows, ND2 position1: HKY+I+G, ND2 position2: GTR+I+G, ND2 position3: GTR+I+G. Four separate runs were set up with four Metropolis-Coupled Markov Chain (**MC3**) Monte Carlo each initiated from random trees and allowed to run for two million generations, sampling every 100 generations. Analyses were terminated when the standard deviation of split frequencies was less than 0.001, the first 25% of trees were discarded as "burn-in", and trees were constructed under 50% majority consensus rule. We obtained ESS values using the Tracer software and confirmed the convergence for all the priors (ESS >200). Support for internal branches in ML and BI trees was quantified using 1000 pseudoreplicates (ultrafast bootstrap **UFB**) and posterior probability (**PP**), respectively. Branch supports (UFB and PP) higher than 95 (UFB: see Minh et al. 2013) and >0.95 were considered as the strong support. The uncorrected pairwise genetic distance (p-distance) was calculated in MEGA v.7 using default settings (pairwise deletion). Genetic divergence between 4–10% is considered moderate and above 10% is considered high.

Species delimitation analyses

We used four distinct approaches Bayesian Poisson Tree Processes (**bPTP**, **PTPML**), Poisson Tree Processes (**PTP**), Automatic Barcode Gap Discovery (**ABGD**), Assemble Species by Automatic Partitioning (**ASAP**) of species delimitation to delimit the number of putative species within our dataset. All the analyses were run in the iTaxoTools (Vences et al. 2021). Settings for each analysis are as follows: bPTP: using the rooted tree with the following options MCMC = 1,000,000, thinning = 100, burn-in = 0.1, seed = 123; ASAP: Substitution model = p-distances, probability = 0.01, best scores = 10, seed value = –1; ABGD: Pmin = 0.001, Pmax = 0.1, steps = 10, X = 1.5, model = Jukes Cantor.

Morphological examination

Measurements were taken using a digital calliper (Mitutoyo) to the nearest 0.1 mm, except tail length which was measured with a thread and a scale. Morphometric and meristic characters were examined with the help of Olympus SZX10 microscope. Morphological terminologies follow Agarwal et al. (2018), otherwise stated as follows. Measurements were taken on the right side of the specimens. The following abbreviations and terminology are used for morphometric measurements and meristic: **SVL**, snout to vent length; **TRL**, trunk length, between the axilla and groin; **BW**, maximum body width; **TL**, tail length, from the cloaca to the tail tip; **TW**, tail width just below spurs; **HL**, head length from the retroarticular process of the jaw to the snout tip; **HW**, maximum head width; **HD**, head depth measured from occiput to throat; **FL**, forearm length, taken from the elbow to the wrist; **CL**, crus length, taken from the knee to the base of the foot; **OD**, orbit diameter, taken between the anterior and posterior bony orbital borders; **NO**, distance between the posterior edge of the nostril and the anterior bony orbital border; **SO**, distance between the snout tip and the anterior bony orbital border; **OE**, distance between the posterior bony orbital border and the anterior border of the ear; **EL**, maximum ear length (horizontal distance); **IN**, minimum internarial distance; **IO**, minimum interorbital distance between left and right supraciliary rows; digits were measured from the proximal apex with the neighbouring digit to the tip (excluding the claw), and numbered from inner (I) to outer (V) as follows: on manus, **FIL**, **FIIL**, **FIIIL**, **FIVL**, **FVL**; on pes, **TIL**, **TIIL**, **TIIIL**, **TIVL**, **TVL**; **PcP**, precloacal pores, a continuous series of pore-bearing scales on the precloacal region that does not extend onto the thighs; **PcFP**, precloacofemoral pores, a continuous series of pore-bearing scales that extends from the precloacal region onto the thighs; **MVSR**, mid-ventral scale rows, counted between ventrolateral folds at the midpoint between axilla and groin; **PVT**, paravertebral tubercles on the trunk, counted between the level of the axilla and the level of the groin; **DTR**, dorsal tubercle rows, counted transversely across the body at the midpoint between axilla and groin; **SL**, total number of supralabials counted on both side; **IL**, total number of infralabials counted on both side. Two separate counts for subdigital lamellae were recorded on fourth digit of the manus and pes of both sides, a count for the basal series, that includes scales of a width at least twice the diameter of palmar and plantar scales up to and including a single large scale at the digital inflection, and a count for the apical series, comprising lamellae distal to the digital inflection but not including the ventral claw sheath and the

small non lamellar scales between the basal and apical lamellae series, abbreviations for lamellae are as follows: on the manus, **FIVLam**; on the pes, **TIVLam**. Sex of the specimens was determined by the presence of hemipenal bulges (male) and absence (female).

Comparative data for the species from the *khasiensis* group were taken from original descriptions and other relevant literature (Jerdon 1870; Bauer 2002, 2003; Li 2007; Mahony 2009; Agarwal et al. 2018a, 2018b; Grismer et al. 2018, 2019; Purkayastha et al. 2020, 2021, 2022; Kamei and Mahony 2021; Liu and Rao 2021; Mahony and Kamei 2021; Bohra et al. 2022; Lalremsanga et al. 2022, 2023; Zhang et al. 2024).

Museum abbreviations

WII-ADR: Wildlife Institute of India, Abhijit Das Reptile Collection, Dehradun, India; **BNHS**: Bombay Natural History Society, Mumbai, India; **NCBS**: National Centre for Biological Sciences, Bengaluru, India; **CES**: Centre for Ecological Sciences, Indian Institute of Sciences, Bengaluru, India.

Results

Molecular analyses and species delimitation analyses

Both Maximum Likelihood and Bayesian inference analyses obtained similar tree topologies. All the sequences included in this study were nested within the *khasiensis* group (Fig. 2), except one sample from Sessni, Arunachal Pradesh that nested together with the *C. kamengensis* Mirza et al., 2022 belonging to the *peguensis* group (Fig. S1). All four clades within the *khasiensis* group (*gansi*, *khasiensis*, *mombergi* and "*cayuensis*") were recovered as strongly supported clades with similar relationship as previously reported.

Samples from Teirei and Phuldungsei of Mizoram nested together with the *C. montanus* (Fig. 2), and samples from Nokrek, Tura peak and Daribokgre of Meghalaya nested together with *C. bapme* (Fig. S1). The recently described *C. arunachalensis* was nested together with the topotypic samples of *C. cayuensis* Li, 2007 and other samples from different parts of Arunachal Pradesh (AP) included in this study (Fig. 2). This subclade was together recovered as sister to a distinct lineage from the Siang valley, AP (Fig. 3A, B) with a strong support in both analyses (PP 1.0 and UFB 100). All the other samples were recovered as distinct lineages within the *khasiensis* group (Fig. 2).

Among the samples included in the study, ABGD, ASAP and mPTP results suggested seven species units, respectively, of which six were congruent with our morphospecies assignments, while the bPTP (IB) suggested eight species. The disagreement between these approaches was mainly the further splitting of subclades 1 and 2 within the *cayuensis* clade (Fig. 2). While ABGD, ASAP and mPTP suggested the subclades 1 and 2 as a single species, bPTP split these into two different units (Fig. 2). However, this split between these two sub clades suggested by bPTP was not morphologically supported. Furthermore, samples from Namdapha Tiger Reserve and Kamlang Tiger Reserve, AP formed two distinct clades and were recovered as distinct units, but with weak morphological and genetic divergence. Based on these suggested results, distinct morphological characteristics (Tables 2, S2) and genetic divergence (Table S3), we here describe six lineages as new species.

cayuensis clade and the validity of *Cyrtodactylus arunachalensis*

The samples from Bodak (Arunachal Pradesh) were recovered as sister to a clade containing samples of *C. cayuensis* + *C. arunachalensis* with strong support (UFB 100, PP 1.0) (Fig. 2). This lineage is described below as a new species. This strongly supported clade (UFB 100, PP 1.0), comprising *C. cayuensis* + *C. arunachalensis* (see below) and the undescribed lineage, was recovered as sister to all the other three clades (*gansi*, *khasiensis* and *mombergi*) with strong support (UFB 100, PP 1.0).

Cyrtodactylus arunachalensis was originally described from the Pakke Tiger Reserve, Arunachal Pradesh, India, based on a series of seven specimens (five males, two females) using molecular and morphological data (Mirza et al. 2021). In the phylogeny presented by Mirza et al. (2021), *C. arunachalensis* was recovered as sister to the *khasiensis* clade, but they did not include samples of *C. cayuensis*. However, in our phylogenetic analyses the samples of *C. arunachalensis* from Mirza et al. (2021) were nested among the topotypic samples of *C. cayuensis* and other samples from different parts of Arunachal Pradesh (Potin, near Diffo River and Ezengo (Mehao Wildlife Sanctuary), Jengging and Ramsing (Mouling National Park), Balek, and near Glaw lake (Kamlang Tiger Reserve) (Fig. 3B). Four largely congruent species delimitation analyses suggest all these samples as a single species unit (Fig. 2). In contrast, bPTP split this clade into two species units that are not congruent with our morphological findings and geographical distribution.

Furthermore, Mirza et al. (2021) did not morphologically compare their new species with *C. cayuensis*, which was once considered a subspecies of *C. khasiensis* (see Agarwal et al. 2018a). In our morphological examination, all diagnostic characteristics have a significant overlap between these two species and the new samples added in this study (Table 2). Interestingly, the precloacal pores in females are reported as absent in both *C. arunachalensis* (n = 2) (Mirza et al. 2021) and *C. cayuensis* (n = 2) (Che et al. 2020) (Table 2). However, precloacal pores were present in all the female specimens (n = 11) that we examined, from this clade, although PcP in females are smaller than that of males (Table S4). Based on the significant morphological overlap, results from the species delimitation anal-

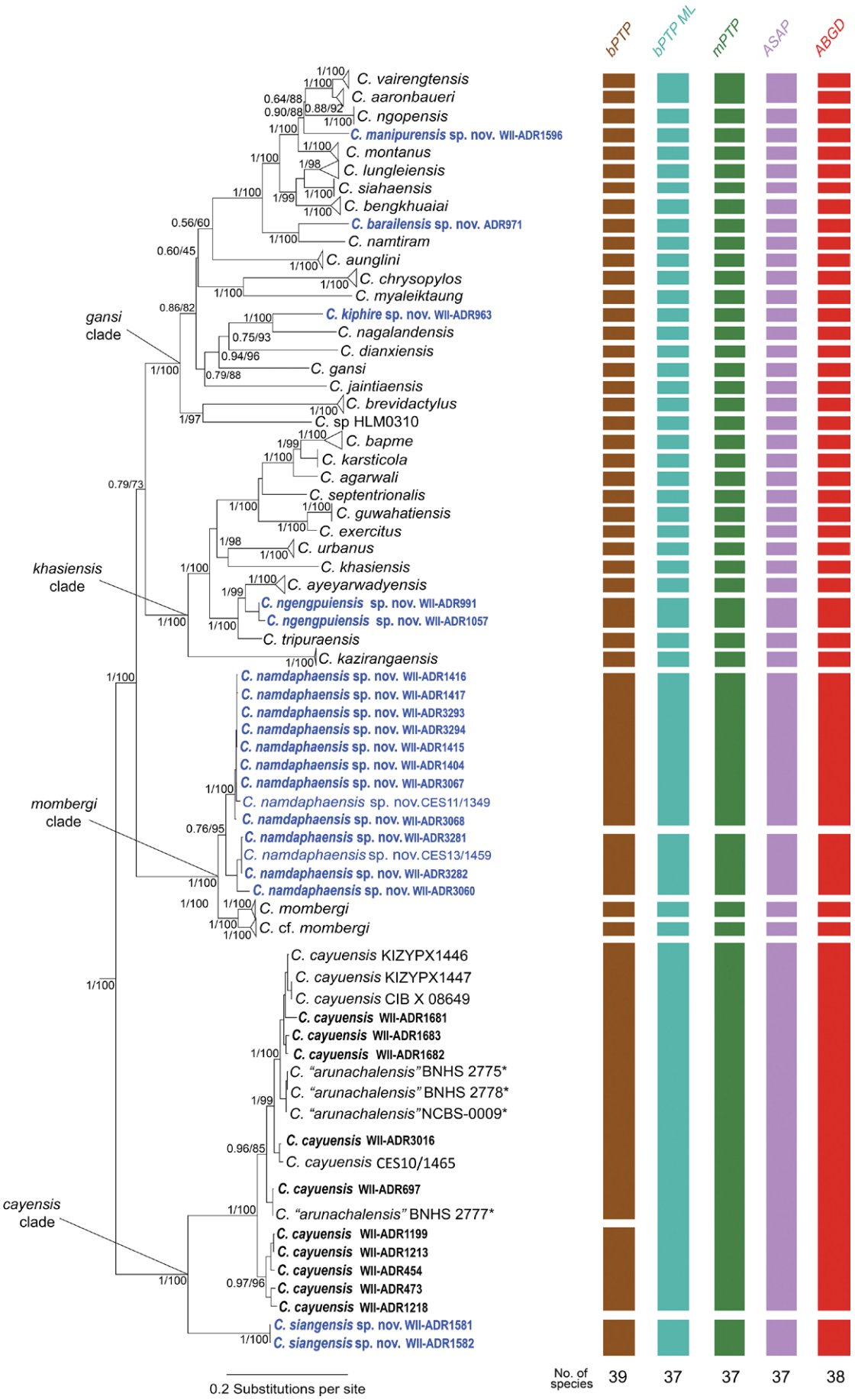

Figure 2. ML phylogeny showing the relationship of the *khasiensis* group. New species described here are marked in blue, other samples generated in this study are in bold. Values in the node represent PP and UFB on the left and right side, respectively. See Fig. S1 for a full tree with outgroups.

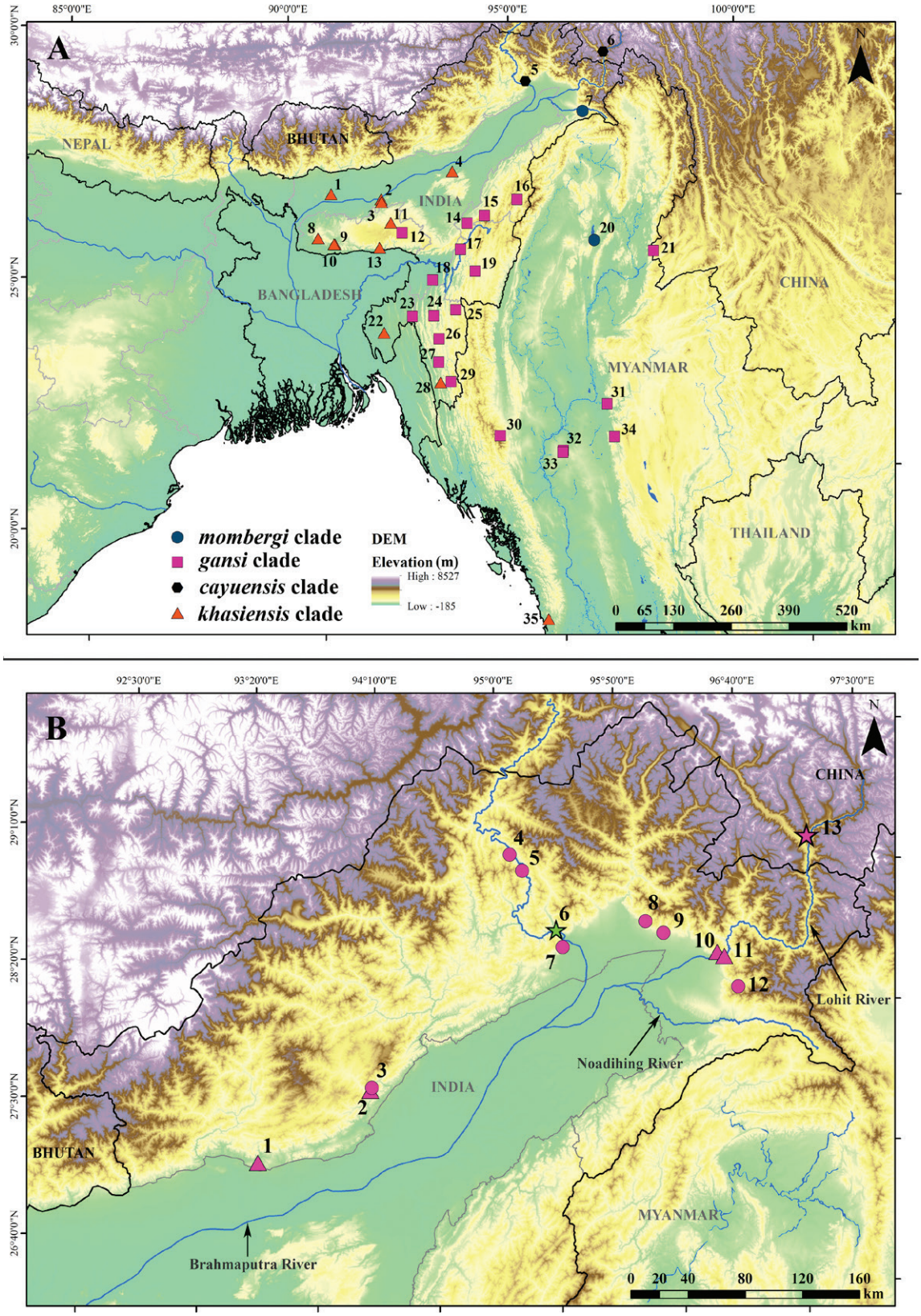

Figure 3. Map showing geographic distribution of the clades within the *khasiensis* group. **A** type localities of the members of the four clades in the Indo-Burma region: **1** *Cyrtodactylus septentrionalis*, **2** *C. guwahatiensis*, **3** *C. urbanus*, **4** *C. kazirangaensis*, **5** *C. siangensis* **sp. nov.**, **6** *C. cayuensis*, **7** *C. namdaphaensis* **sp. nov.**, **8** *C. bapme*, **9** *C. karsticola*, **10** *C. agarwali*, **11** *C. exercitus*, **12** *C. jaintiaensis*, **13** *C. khasiensis*, **14** *C. barailensis* **sp. nov.**, **15** *C. nagalandensis*, **16** *C. kiphire* **sp. nov.**, **17** *C. namtiram*, **18** *C. vairengtensis*, **19** *C. manipurensis* **sp. nov.**, **20** *C. mombergi*, **21** *C. dianxiensis*, **22** *C. tripuraensis*, **23** *C. montanus*, **24** *C. aaronbaueri*, **25** *C. bengkhuaiai*, **26** *C. ngopensis*, **27** *C. lungleiensis*, **28** *C. ngengpuiensis* **sp. nov.**, **29** *C. siahaensis*, **30** *C. gansi*, **31** *C. myaleiktaung*, **32** *C. brevidactylus*, **33** *C. aunglini*, **34** *C. chrysopylos*, **35** *C. ayeyarwadyensis*; **B** *cayuensis* clade, **green star** (type locality of *C. siangensis* **sp. nov.**), **pink star** (type locality of *C. cayuensis*), **pink triangle** (*C.* "*arunachalensis*"), **pink circle** (*C. cayuensis* recorded in this study) (numbers correspond to the locality given in Table 1).

Table 2. Comparative table of summary morphological characteristics among the members of the *khasiensis* group including the seven new species. NA- data not available; "*" data from the literature is not comparable with our data as the count method is different.

Species	SVL (mm) Male	SVL (mm) Female	SL	IL	PcP (male)	PcP (female)	PcFP (male)	DTR	PVT	MVSR	Enlarged Plate like Subcaudal	Ventrolateral Fold	Lam FIV	Lam TIV	Reference
C. dianxiensis	73.8–79.9	75	9–12	8–11	7–8	0	0	17–19	31 or 32	35–41	no	present	16 or 17	19–20	Liu and Rao (2021), Zhang et al. (2024)
C. tamaiensis	90	NA	10	9	0	NA	40	21	*	37	no	present	16	16	Mahony (2009)
C. mandalayensis	61.7	NA	10/ 12	9/ 10	8	NA	0	18	*	32	no	present	12	18	Mahony (2009)
C. ngopensis	62.6–66.8	64.9–68.6	10–11	9–11	6	0–6 pitted scales	0	19 or 20	32–36	32–39	no	present	11–15	14–18	Bohra et al. (2022)
C. vairengtensis	58.8–68.4	57.6–73.6	10–11	10–11	9–11	5–9 pitted scales	0	22 or 23	34–39	35–41	no	present	12–16	14–17	Lalremsanga et al. (2023)
C. namtiram	65.8	NA	8/9	10	12	NA	0	21	33	36	no	present	14	17	Mahony and Kamei (2021)
C. mombergi	66.5–67.4	64–74	*	*	10 or 11	0–9	0	23–27	35–42	31–39	no	present	NA	19–22	Grismer et al. (2019)
C. aunglini	68.6–81.6	NA	*	*	12 or 13	NA	0	21–26	37–45	41–47	no	present	NA	19–23	Grismer et al. (2018); and Mahony and Kamei (2021) for corrected characters
C. myaleiktaung	NA	67.4	*	*	NA	0	0	NA	NA	57	NA	present	NA	18	Grismer et al. (2018)
C. brevidactylus	71.4	84.3–88.0	10–12	10–11	8	8	0	27–30	38–42	35–46	no	absent	NA	18 or 19	Bauer (2002), Grismer et al. (2018)
C. chrysopylos	64.9–79. 1	66.7–83.8	*	*	8–13	0	0	16–20	30–35	37–55	no	present	NA	19–23	Bauer (2002), Grismer et al. (2018)
C. lungleiensis	65.0–68.1	64.9–75.1	10–11	9–11	3–5	5–7 pitted scales	0	24–28	32–40	37–43	no	present	13 or 15	16–18	Lalremsanga et al. (2022)
C. exercitus	48.1–68.0	66.7	9–11	9–10	11–15	11 pitted scales	0	21–24	32–34	35–37	no	present	14–16	16–17	Purkayastha et al. (2022)
C. siahaensis	57.3–61.1	42.6–72	9–11	9–11	7	0–3 pitted scales	0	22–24	36–39	34–37	no	present	13 or 14	15–18	Purkayastha et al. (2022)
C. bapme	NA	69.9–77.0	8–12	8–10	0	0–13 pitted scales	NA	21–24	32–37	30–39	no	present	12–19	15–22	Kamei and Mahony (2021)
C. karsticola	63.7–69.1	70.7	10–11	9–10	0	13 pitted scales	34–38	21–24	34–39	35–39	no	present	16	15–18	Purkayastha et al. (2021)
C. agarwali	56.4–71.8	NA	9–12	8–10	11–18	NA	0	21–25	34–38	32–39	no	present	15–17	15–19	Purkayastha et al. (2021)
C. aaronbaueri	54.2–61.1	61.8–69.5	8–11	8–12	7–8	6–8 pitted scales	0	22–28	36–39	35–40	no	present	12–14	14–19	Purkayastha et al. (2021)
C. bengkhuaiai	62.5–63.9	54.9–72.5	9–11	7–11	5–7	4–5 pitted scales	0	22–26	35–41	37–42	no	present	13–16	15–19	Purkayastha et al. (2021)

Species	SVL (mm) Male	SVL (mm) Female	SL	IL	PcP (male)	PcP (female)	PcFP (male)	DTR	PVT	MVSR	Enlarged Plate like Subcaudal	Ventrolateral Fold	Lam FIV	Lam TIV	Reference
C. cayuensis	80 (max value)		9–12	8–11	6–9 (irrespective of sex)	0	0	*	*	28–34	NA	MA	NA	NA	Li (2007)
C. cayuensis (Tibet)	63	72–79	*	*	6–8	0	0	18	*	28–34	no	present	NA	NA	Che et al. (2020)
C. cayuensis (= arunachalensis)	64.8–83.5	74.9–81.7	8–11	8–10	6–10	0	0	24–26	*	~38	no	present	15–21	15–23	Mirza et al. (2021)
C. cayuensis (newly collected materials from India)	61.2–75.1	59.4–83.6	9–13	8–12	7 or 9	7–10	0	15–21	27–38	34–44	no	present	13–17	11–21	This study
C. urbanus	65.4–71.9	73.3–75.6	8–11	8–10	9–13	0	0	20–24	30–40	30–39	no	present	15–19	17–21	Purkayastha et al. (2020), Kamei and Mahony (2021)
C. guwahatiensis	61.9–69.6	69.8–70.5	8–11	8–10	0	0	26–39	21–24	35–38	30–35	no	present	15–18	13–16	Agarwal et al. (2018b), Purkayastha et al. (2020)
C. kazirangaensis	74.8–80.0	NA	11 or 12	9–11	10 or 11	NA	0	22 or 23	36–38	37–43	no	present	15 or 18	14–19	Agarwal et al. (2018b)
C. jaintiaensis	87.0–88.3	96.2	8 or 9	9 or 10	11 or 12	12	0	19 or 20	30–34	40 or 42	no	present	16 or 19	15–18	Agarwal et al. (2018b)
C. montanus	53.6–55.0	58.8–78.2	8 or 10	8–10	8–10	0	0	21–23	37–43	36–42	no	present	12–16	13–18	Agarwal et al. (2018b)
C. nagalandensis	NA	67.5–72.0	10–12	8–10	NA	6 scales with depression	0	16–18	35–37	34 or 35	no	present	12 or 14	16	Agarwal et al. (2018b)
C. septentrionalis	58	65.2	9 or 10	9	14	14 indistinct depressions	0	23 or 24	38–42	35–38	no	present	15	15–20	Agarwal et al. (2018b)
C. khasiensis	57.0–80.0	72.1–81.1	9–13	8–11	10–12	0	0	19–23	*	34–42	yes	present	12–21	13–23	Agarwal et al. (2018a)
C. tripuraenensis	54.4–63.7	57.5–70.7	8–12	8–10	0	0	29–37 (male), 19–29 (female)	19–21	*	35–43	no	present	16–23	16–27	Agarwal et al. (2018a)
C. gansi	46.5–62.3	62.4	*	*	16–29	13	0	20–25	NA	36–40	no	absent	NA	NA	Bauer (2003)
C. ayeyarwadyensis	62.1–67.6	64.1–71.8	*	*	10–28	0	0	22–24	NA	32–37	no	present	NA	NA	Bauer (2003)
C. ngengpuiensis **sp. nov.**	61.2	53.9–74.1	9–12	8–11	0	10–16	27	18 or 20	29–34	38 or 39	no	present	11–14	12–16	This study
C. barailensis **sp. nov.**	NA	68.8	9 or 12	9	NA	10	0	17	32	36	no	present	12 or 13	17	This study
C. namdaphaensis **sp. nov.**	57.5–70.7	54.8–69.3	8–11	8–11	7–9	8–10	0	17–19	29–36	33–40	no	present	12–15	11–17	This study
C. kiphire **sp. nov.**	63.9–64.7	NA	10	9–12	6 or 7	NA	0	16	26 or 29	35 or 36	no	present	12 or 13	12–14	This study
C. manipurensis **sp. nov.**	59.5	NA	10	8 or 9	7	NA	0	21	37	36	no	present	11 or 12	13 or 16	This study
C. siangensis **sp. nov.**	NA	70.1–72.1	8–12	9–12	NA	8 or 10	0	15 or 16	26–32	40–45	no	present	13–17	14–19	This study

yses and low genetic divergence, we consider this clade to represent be composed of a single species. Hence, we herein provide an extended description for *C. cayuensis* and propose to treat that *C. arunachalensis* as is a junior subjective synonym of *C. cayuensis*. Consequently, we also propose to refer to this clade consisting of *C. cayuensis* and *C. siangensis* **sp. nov.** as *cayuensis* clade.

Systematics

gansi clade

This clade was recovered as a strongly supported monophyletic group in both analyses (UFB 100, PP 1.0) comprising 16 described species and four undescribed lineages. All the members of this lineage are distributed south of Brahmaputra River in the Indo-Burma region (sensu Grismer et al. 2022). Among the samples included in this study, the samples from Lamdan Kabui of Manipur and Athibung and Kiphire of Nagaland clustered with this clade representing distinct lineages. The sample from Lamdan Kabui is here recovered as sister to *C. ngopensis*, *C. aaronbaueri* and *C. vareingtensis* with moderate support in ML (UFB 88) and in BI (PP 0.90) (Fig. 2). The sample from Athibung is recovered as sister to *C. namtiram* with strong support in both analyses (UFB 100, PP 1.0) and the sample from Kiphire was recovered as sister to *C. nagalandensis* with strong support in both analyses (UFB 100, PP 1.0). All these three lineages were recovered as distinct species units in all our species delimitation analyses. The morphological descriptions of these three lineages are provided below.

Diagnosis. Members of the *gansi* clade can be diagnosed by the following set of morphological characters: SVL 46.5–88.3 mm in adult males and SVL 42.6–96.2 mm in adult females; 8–12 supralabials; 7–12 infralabials; 16–30 dorsal tubercle rows on mid-dorsum; 26–45 paravertebral tubercles between the level of axilla and groin; 32–57 mid-ventral scales; 3–29 precloacal pores in males; precloacal pores in females may be absent, or 3–8 pitted precloacal scales or 8–13 precloacal pores present; ventrolateral skin fold present except in *C. gansi*; 11–19 subdigital lamellae on fourth finger; 12–23 subdigital lamellae on fourth toe.

Cyrtodactylus kiphire Boruah, Narayanan, Deepak & Das sp. nov.

https://zoobank.org/ECA0B2C2-D3C2-4C26-AA46-320CBD36AE06

Figure 4; Tables 2, S2

Holotype. Adult male (WII-ADR964; Fig. 4A–E), from a trail beside Forest Colony (25.8994°N; 94.7694°E; elevation 1300 m a.s.l.; Fig. 3A), Kiphire Forest Division, Kiphire District, Nagaland, India; collected by Abhijit Das and Bitupan Boruah on 1 August 2021.

Paratype. An adult male (WII-ADR963; Fig. 4F, G) collection locality details are same as the holotype.

Diagnosis. A medium-sized gecko (SVL up to at least 64.7 mm); 10 supralabials; 9–12 infralabials; 16 bluntly conical and feebly keeled dorsal tubercles; 26–29 paravertebral tubercles; 35 or 36 midventral scales rows between the weak ventrolateral folds; no precloacal groove; six or seven precloacal pores in continuous series; 12–15 total subdigital lamellae beneath digit IV of pes; dark brown irregular cross bars or reticulation on dorsum.

Description of the holotype. Holotype well preserved except single incision below left axilla ventrolaterally. Snout-vent length 63.9 mm. Head moderately large (HL/SVL = 0.26), dorsoventrally depressed, longer than width (HW/HL = 0.68), distinct from neck, broader at occipital region; snout tip rounded in both dorsal and lateral view; loreal region convex; canthus rostralis rounded, indistinct; interorbital space flat; a longitudinal furrow on dorsal surface of the snout; snout short (SO/HL = 0.4), longer than orbit (OD/SO = 0.7); nostril nearly rounded, opening directed posterolaterally; ear opening oval and oblique; scales on head heterogeneous, largest on snout and loreal region, posteriorly smaller in upper eyelid, interorbital space and occipital region, granular juxtaposed; scales on upper eyelids heterogeneous, supraciliaries outwardly sharp giving serrated appearance in dorsal view, size anteriorly and posteriorly decreases, largest at approximately anterior one third of it; rostral wide, a short groove at the middle on top; rostral connected with nasals, supranasals, internasal and first supralabials; two scale between the supranasals, larger than the rest of the granular snout scales; granular scales at parietal region and occipital region intermixed with slightly large rounded granular tubercles starting from the level of posterior margin of the upper eyelids, size increases towards nape; supralabial 10 on both side, seven supralabials upto midorbit, size decreases towards angle of jaw; a series of narrow, enlarged scales above the supralabials between nostril and anterior orbital border; mental slightly wider than rostral (RW/MW = 0.8), triangular, connected with first infralabials, inner postmentals; nine infralabials on both sides, size decreases towards angle of jaw; first infralabials connected with mental, second infralabial, inner and outer postmentals; inner pair of postmentals are larger than the outer postmentals; posterior margin of the inner postmentals bordered by eight granular scales of different size; two rows of enlarged scales along the infralabials starting below the outer postmentals, posteriorly size decreases, elongated and narrow; rest of the gular scales are small, granular juxtaposed, homogeneous, size increases towards the throat where they become imbricate.

Habitus slender (BW/SVL = 0.2, TRL/SVL = 0.35), dorsoventrally depressed; dorsal scales granular, rounded, heterogeneous, intermixed with rounded, weakly

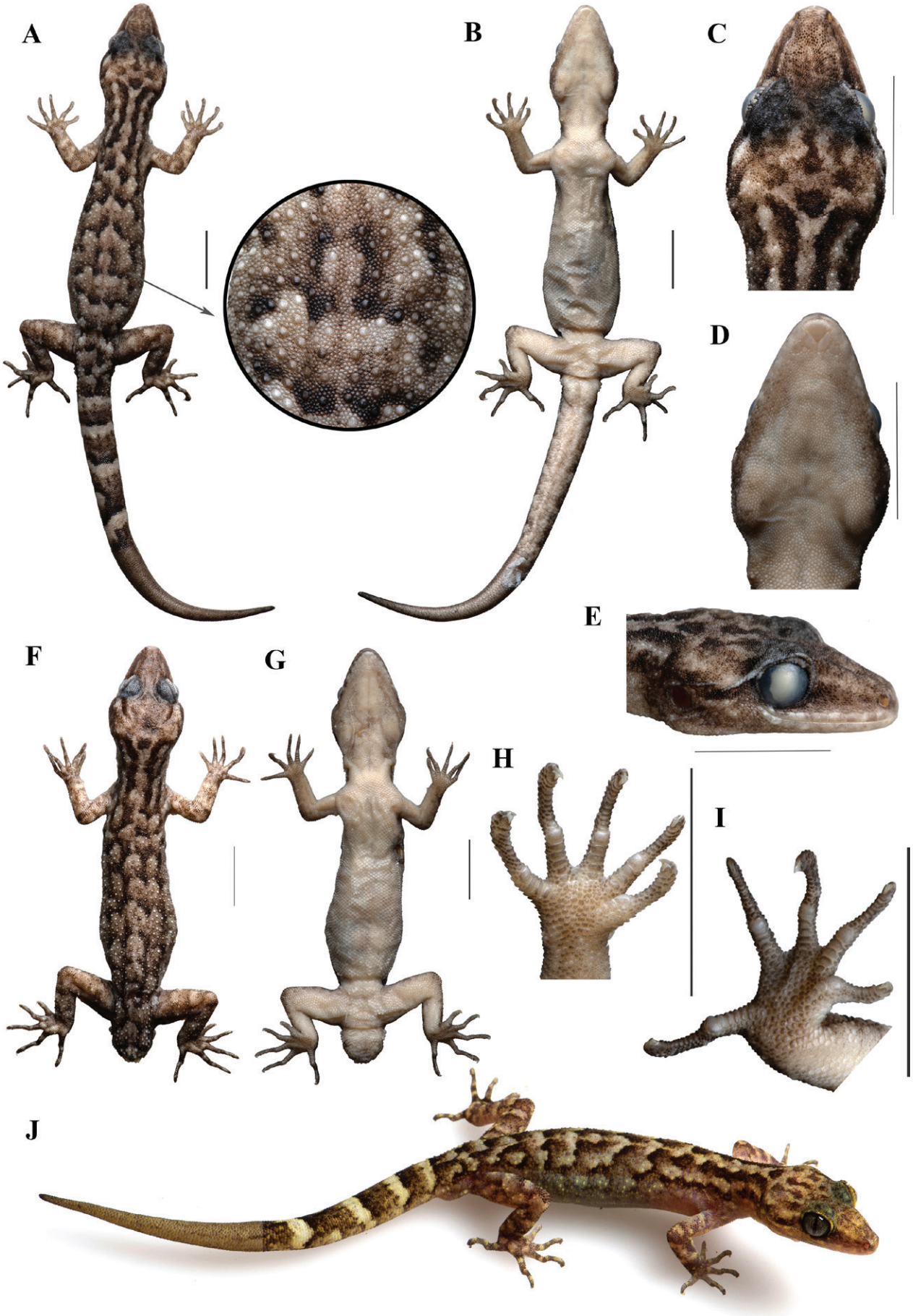

Figure 4. *Cyrtodactylus kiphire* **sp. nov. A**–**E** holotype (WII-ADR964), **A** dorsal view, **B** ventral view, **C** dorsal view of head, **D** ventral view of head, **E** lateral view of head; **F**, **G** dorsal and ventral view of paratype (WII-ADR963); **I** ventral view of right manus and **J** right pes (WII-ADR964); **K** holotype in life. Scale bar: 10 mm. **J** not to scale.

keeled and bluntly conical tubercles irregularly arranged, up to fourth segment of the tail, size increases towards posterior body and pronounced; 16 dorsal tubercles across mid dorsum; 26 paravertebral tubercles; ventrolateral fold weak; ventral scales larger than those of dorsal, flat, smooth, cycloid subimbricate to imbricate, largest on belly; 36 mid-ventral scales between ventrolateral fold; seven precloacal pores arranged in an inverted "V" shaped continuous series, followed by five unpored, large scales below it, largest at the apex.

Forelimbs and hindlimbs slender (FL/SVL = 0.13, CL/SVL = 0.16); digits strongly inflected at the joints, all bearing large recurved claw, enlarged subdigital lamellae; lamellae beneath digit IV of right and left manus (given as basal + distal) is 5+8 and 5+9 respectively; lamellae beneath digit IV of right and left pes (given as basal + distal) is 5+10 and 5+9 respectively; dorsal scales on forelimbs smooth and subimbricate, small and granular at elbow and proximal end of forearm; forearm scales intermixed with rounded large tubercles; dorsal scales of hindlimbs heterogeneous, intermixed with large, rounded and bluntly conical tubercles; horizontally upper half of the thigh scales are smooth, large and subimbricate, those on lower half small granular; scales on tibia are small, granular juxtaposed; ventral scales of forelimbs granular, juxtaposed, mostly homogeneous; scales on palm heterogeneous in shape and size, granular juxtaposed; scales on ventral side of hindlimbs smaller than those of belly, smooth, cycloid and subimbricate, but on the knee, above cloaca and on thigh below the level of precloacal pores are smaller and granular; scales on soles heterogeneous, granular, juxtaposed to subimbricate.

Tail regenerated (TL = 68 mm), slender, gradually tapering towards tip, segments indistinct, dorsal scales small, granular, juxtaposed at the base, posteriorly size increases, flat, smooth, subimbricate, heterogeneous in shape and size; large feebly keeled scales upto fourth segment of the tail, those on basal segment are pronounced; subcaudal scales smooth, subimbricate, wider than that of dorsal and widest at the middle, heterogeneous in shape and size; no enlarged plate like series of subcaudal scales; two and three bluntly conical spurs on right and left side of the tail base respectively.

Colouration in life. Top of head intermixed with pale-yellow and pale-brown; dark-brown spots of irregular shape and size on posterior part of head; short dark-brown postorbital streak present; another streak along loreal region; supraciliary yellow; four dark-brown stripes on neck interspaced with cream colour; large spot at the middle on the anterior part of the nape; six dark-brown cross bars of irregular size and shape on dorsum between the level of axilla and groin (Fig. 4J); these cross bars intersected on mid dorsum and posteriorly bordered with cream coloured patches; limbs with slightly dark-brown indistinct reticulations intermixed with pale-yellow or cream coloured patches; scales on axillary region and base of forelimbs are with pinkish tinge; digits with alternating brown and pale-yellow bands; anterior half of the tail with alternating dark-brown and light-cream coloured cross bands of irregular shape and size; posterior half (regenerated part) of the tail pale-brown; ventrally head, trunk and limbs whitish; tail with brown mottling.

Colouration in preservative. Top of head, back, limbs and tail pale-greyish-brown with dark-brown markings; upper eyelids grey; dorsal marking pattern as it was in life; and ventrally whitish.

Morphological variation. Detailed morphometric variations are given in Table S2. Apart from those, the dorsal colour and marking pattern of the paratype varied from that of holotype. Paratype has two post orbital streaks on each side, upper one shorter than the lower one; no other spots on occipital region as in the holotype; dorsal cross bands somewhat reticulated (Fig. 4F).

Comparison. *Cyrtodactylus kiphire* **sp. nov.** differs from *C. aaronbaueri* by having larger body size in male, SVL 63.9–64.7 mm (vs. SVL 54.2–62 mm in male), fewer dorsal tubercle rows, DTR 16 (vs. DTR 22–28), fewer paravertebral tubercles, 26–29 (vs. PVT 36–39); differs from *C. aunglini* by fewer dorsal tubercle rows, DTR 16 (vs. DTR 21–26), fewer precloacal pores, PcP 6 or 7 (vs. PcP 12–13), fewer mid-ventral scale rows, MVSR 35 or 36 (vs. MVSR 41–49), fewer paravertebral tubercles, PVT 26–29 (vs. 36–45); differs from *C. bengkhuaiai* by fewer dorsal tubercle rows, DTR 16 (vs. DTR 22–26), fewer paravertebral tubercles, 26–29 (vs. PVT 35–41), fewer mid-ventral scale rows, MVSR 35 or 36 (vs. MVSR 37–42); differs from *C. brevidactylus* by fewer dorsal tubercle rows, DTR 16 (vs. DTR 27), fewer mid-ventral scale rows, MVSR 35 or 36 (vs. MVSR 45), fewer precloacal pores, PcP 6 or 7 (vs. PcP 8); differs from *C. chrysopylos* by fewer precloacal pores, PcP 6 or 7 (vs. PcP 8–13), mid ventral scales, MVSR 35 or 36 (vs. MVSR 37–55), dorsal tubercle rows, DTR 26–29 (vs. DTR 30–35); differs from *C. dianxiensis* by smaller body size, SVL 63.9–64.7 mm (vs. SVL 73.8–79.9 mm), fewer dorsal tubercle rows, DTR 16 (vs. DTR 18 or 19), 35 or 36 mid ventral scales (vs. MVSR 37–41), 26 or 29 paravertebral tubercles (vs. PVT 31 or 32); differs from *C. gansi* by fewer dorsal tubercle rows, DTR 16 (vs. DTR 20–25), having fewer precloacal pores, PcP 6 or 7 (vs. PcP 16–29); differs from *C. jaintiaensis* by smaller body size in male, SVL 63.9–64.7 mm (vs. SVL 87–88.3 mm), fewer dorsal tubercle rows, DTR 16 (vs. DTR 19–20), fewer mid-ventral scale rows, MVSR 35 or 36 (vs. MVSR 40–42), fewer precloacal pores, PcP 6 or 7 (vs. PcP 11–12); differs from *C. lungleiensis* by smaller body size in male, SVL 63.9–64.7 mm (vs. SVL 65–68.1 mm), higher precloacal pores, PcP 6 or 7 (vs. PcP 3–5), fewer mid-ventral scale rows, MVSR 35 or 36 (vs. MVSR 37–43), fewer dorsal tubercle rows, DTR 16 (vs. 24–28), fewer paravertebral scales, PVT 26–29 (vs. 32–40), fewer subdigital lamellae beneath toe IV, TIVLam 12–14 (vs. TIVLam 16–18); differs from *C. montanus* by larger body size in male, SVL 63.9–64.7 mm (vs. SVL 53.6–55 mm), fewer dorsal tubercle rows, DTR 16 (vs. DTR 21–23), fewer precloacal pores, PcP 6 or 7 (vs. PcP 8–10); differs from *C.*

myaleiktaung by fewer mid-ventral scale rows, MVSR 35 or 36 (vs. MVSR 57); differs from *C. namtiram* by fewer dorsal tubercle rows, DTR 16 (vs. DTR 21), fewer number of paravertebral scales, PVT 26–29 (vs. PVT 33), fewer precloacal pores, PcP 6 or 7 (vs. PcP 12); differs from *C. ngopensis* by fewer dorsal tubercle rows, DTR 16 (vs. 19–20), fewer paravertebral tubercles, PVT 26–29 (vs. 32–36); differs from *C. siahaensis* by fewer dorsal tubercle rows, DTR 16 (vs. DTR 22–24), fewer paravertebral tubercles, 26–29 (PVT 36–39); differs from *C. vairengtensis* by fewer dorsal tubercle rows, DTR 16 (vs. 22–23), fewer paravertebral tubercles, PVT 26–29 (vs. 34–39), fewer precloacal pores in male, PcP 6 or 7 (vs. PcP 9–11). The new species is morphologically close to *C. nagalandensis*; however, the new species differs from it by fewer paravertebral tubercles, PVT 26–29 (vs. 35–37). We could not compare with male specimens as data for *C. nagalandensis* is not available. Morphological differences with other members of *khasiensis* group is presented in Table 2.

Sequence divergence. *Cyrtodactylus kiphire* **sp. nov.** has a high genetic divergence of 12% from its closely related *C. nagalandensis*, 16.3% from *C. dianxiensis*, 16.9% from *C. gansi* and 17.9% from *C. jaintiaensis*. With other members of the clade, *C. kiphirie* **sp. nov.** has a genetic divergence of 16.4% and 22.5% in the ND2 gene (Table S3).

Etymology. The specific epithet is derived from Kiphire, a District of Nagaland from where the type series of this species were collected.

Suggested common name. Kiphire bent-toed gecko.

Distribution and natural history. We recorded *Cyrtodactylus kiphire* **sp. nov.** from Kiphire forest colony, Kiphire District, Nagaland, India. The area is characterised as subtropical forest with regenerating jhum forest dominated by *Castanopsis indica* (Roxb. ex Lindl.) A. DC., *Quercus* sp., *Itea macrophylla* Wall. ex Roxb., *Albizia chinensis* (Osbeck) Merr.. The holotype was collected from on a forest trail shrub (approximately 2.0 m from the ground) at approximately 23:00 hrs. The paratype was collected from a rocky slope along the edge of a stream.

Cyrtodactylus barailensis Boruah, Narayanan, Deepak & Das sp. nov.

https://zoobank.org/6196FFDC-ED56-484E-A845-0C0A7D542BF9

Figure 5; Tables 2, S2

Holotype. Adult female (WII-ADR971), from Athibung (25.54199°N; 93.6307°E; elevation 740 m a.s.l.) (Fig. 3A), Peren District, Nagaland, collected by Abhijit Das and Bitupan Boruah on 14 August 2021.

Diagnosis. Medium-sized gecko, SVL at least 68.8 mm in adult female; supralabials 9–12 and infralabials nine; 12 or 13 lamellae beneath the digit IV of manus; 17 lamellae beneath digit IV of pes; 17 feebly keeled and bluntly conical tubercles across mid dorsum and 32 paravertebral tubercles; 36 smooth mid-ventral scales between ventrolateral folds; at least 10 small precloacal pores in female; head on top pale-brown with purplish tinge; dark-brown postorbital stripe continuing to above the ear opening; a dark-brown cross bar with irregular edges on nape; indistinct pale-yellow patch on occipital region; dorsally and laterally neck and back pale yellowish-brown with dark-brown irregular reticulation.

Description of holotype. Holotype well preserved except an incision below left axilla ventrolaterally. Snout-vent length 68.8 mm. Head moderately large (HL/SVL = 0.26), dorsoventrally depressed, longer than width (HW/HL = 0.65), oval, distinct from neck, broader at occipital region; snout tip rounded in both dorsal and lateral view; loreal region convex; canthus rostralis rounded, indistinct; interorbital space flat; a longitudinal furrow on dorsal surface of the snout; snout short (SO/HL = 0.39), longer than orbit (OD/SO = 0.59); nostril rounded, opening directed posterolaterally; ear opening oblique; scales on head heterogeneous, largest on snout and loreal region, posteriorly smaller in upper eyelid, interorbital space and occipital region, granular juxtaposed; scales on upper eyelids heterogeneous, supraciliaries outwardly sharp giving serrated appearance in dorsal view, size anteriorly and posteriorly decreases, largest at the anterodorsal region; rostral wide, a short groove at the middle on top; rostral connected with nasals, supranasals and first supralabials; a single scale between the supranasals, larger than the rest of the granular snout scales; granular scales at parietal, occipital and temporal region intermixed with slightly larger rounded and bluntly conical granular tubercles starting from the level of posterior margin of the upper eyelids, smaller in parietal region, size increases towards nape; supralabial 12 on right side and nine on left side, supralabials count up to midorbit is eight on right side and six on left side, size decreases towards angle of jaw; a series of narrow, enlarged scales above the supralabials between nostril and anterior orbital border; mental triangular, connected with first infralabials and inner postmentals; nine infralabials on both side, size decreases towards angle of jaw; inner pair of postmentals are larger than the outer postmentals; posterior margin of the inner postmentals bordered by eight granular scales of different size; two rows of slightly enlarged, narrow scales, larger than gular scales present along the infralabials starting below the outer postmentals, posteriorly size decreases; gular scales granular, juxtaposed, homogeneous, size increases towards the throat where they become imbricate.

Habitus slender (BW/SVL = 0.16, TRL/SVL = 0.47), dorsoventrally depressed; dorsal scales granular, rounded, heterogeneous, intermixed with densely placed rounded, weakly keeled and bluntly conical tubercles, irregularly arranged, continues to seventh segment of the tail, size increases towards posterior body and pronounced at the

Figure 5. Holotype of *Cyrtodactylus barailensis* **sp. nov.** (WII-ADR971). **A** dorsal and **B** ventral view of the whole body; **C** dorsal, **D** ventral, and **E** lateral view of head; **F** dorsal tubercles on trunk; **G** ventral view of left manus, and **H** left pes. **I** *C. barailensis* **sp. nov.** in life. Scale bar: 10 mm.

base of tail; 17 dorsal tubercles across mid dorsum; 32 paravertebral tubercles; ventrolateral fold weak; ventral scales larger than those of dorsal, flat, smooth, cycloid, subimbricate to imbricate, largest on posterior part of the belly, 36 mid-ventral scales between ventrolateral folds; 10 small precloacal pores arranged in an inverted "V" shaped continuous series, followed by a series eight unpored, enlarged scales below it.

Forelimbs and hindlimbs slender (FL/SVL = 0.14, CL/SVL = 0.18); digits strongly inflected at the joints, all bearing large recurved claw and enlarged subdigital lamellae; lamellae count beneath digit IV of right and left manus (given as basal + distal) is 5+7 and 5+8 respectively; lamellae count beneath digit IV of both right and left pes (given as basal + distal) is 8+9; dorsal scales on forelimbs heterogeneous in size; hind arm scales smooth and subimbricate; forearm scales small and granular towards proximal and towards distal end it is smooth, cycloid and imbricate; forearm scales intermixed with enlarged feebly keeled tubercles; dorsal scales of hindlimbs heterogeneous, intermixed with densely placed large, rounded and bluntly conical tubercles; scales on inner lateral and dorsolateral side of the thighs smooth, large and imbricate, rest of the scales are granular; scales on tibia are small, granular juxtaposed; ventral scales of forelimbs granular, juxtaposed, mostly homogeneous; scales on palm heterogeneous in shape and size, granular juxtaposed; ventral scales of hind limbs smaller than those of belly, smooth, cycloid and subimbricate; scales on the knee, above cloaca and on thigh below the level of precloacal pores smaller and granular; scales on soles heterogeneous, granular, juxtaposed to subimbricate.

Tail complete, posterior 6 mm regenerated (TL = 64 mm), slender, gradually tapering towards tip; tail segments indistinct; dorsal scales small, granular, juxtaposed at the base, posteriorly size of the scales increases, flat, smooth, subimbricate, heterogeneous in shape and size; enlarged feebly keeled scales up to seventh segment of the tail, those on basal segment are pronounced; subcaudal scales smooth, subimbricate, wider than that of dorsal, heterogeneous in shape and size; no enlarged plate like series of subcaudal scales; four bluntly conical spurs on both sides of the tail base.

Colouration in life. Head on top pale-brown with purplish tinge, indistinct brown irregular spots on occipital region; a short brown streak behind the posterior corner of the upper eyelid; a broad, dark-brown postorbital stripe continuing to above the ear opening; area between these two postorbital streaks is paler than dorsal head colour; an indistinct brown loreal stripe covering the nasal and an indistinct pale stripe above it; indistinct pale-yellow patch on occipital region; lips and mandibular region paler with indistinct yellow spots; dorsally and laterally neck and back pale yellowish-brown with dark-brown irregular reticulation starting from neck to sacrum; a dark-brown cross bar with irregular edges on nape; limbs pale-yellowish-brown with dark-brown reticulation; digits with alternative dark-brown and pale-yellow bars; tail with alternative 11 dark and 10 light bars in the original part, dark bars posteriorly more darker and broader; light bars posteriorly more whitish, first bar at the base of tail broken into two spots; fourth and fifth bar connected on left side; ventrally head, trunk and limbs whitish; tail with irregular brown and pale-yellow patches (Fig. 5I).

Colouration in preservative. Top of head pale-greyish-brown; neck, back, limbs and tail dorsally light-grey with dark-brown markings; marking pattern visible as those in life condition; ventrally whitish with brown specks on tail.

Comparison. *Cyrtodactylus barailensis* **sp. nov.** differs from *C. aaronbaueri* by fewer dorsal tubercle rows, DTR 17 (vs. DTR 22–28), 10 precloacal pores (vs. 6–8 pitted precloacal scales in female); differs from *C. agarwali* by fewer dorsal tubercle rows, DTR 17 (vs. 21–25); differs from *C. aunglini* by fewer mid-ventral scale rows, MVSR 36 (vs. MVSR 47–49), 32 paravertebral tubercle (vs. PVT 36–45), 17 dorsal tubercle rows (vs. DTR 21–26); differs from *C. bengkhuaiai* by having fewer dorsal tubercle rows, DTR 17 (vs. DTR 22–26), 10 precloacal pores (vs. 6–8 pitted precloacal scales in females); differs from *C. brevidactylus* by fewer dorsal tubercle rows, DTR 17 (vs. DTR 27–30), fewer paravertebral tubercles, PVT 32 (vs. PVT 38–42), enlarged dark blotches on head and dorsum absent (vs. large dark blotches on dorsum between nape and sacrum); differs from *C. chrysopylos* by presence of precloacal pores (vs. PcP absent in female), fewer mid-ventral scales, MVSR 36 (vs. MVSR 37–55); differs from *C. dianxiensis* by smaller body size, SVL 68.8 mm (vs. SVL 75 mm), presence of precloacal pores (vs. PcP absent in female), fewer subdigital lamellae, 12 or 13 under fourth finger and 16 under fourth toe (vs. 16 or 17 under fourth finger and 19 or 20 under fourth toe); differs from *C. gansi* by fewer dorsal tubercle rows, DTR 17 (vs. DTR 20–25), ventrolateral fold present on trunk (vs. absent), fewer precloacal pores, PcP 10 (vs. PcP 13 in female); differs from *C. jaintiaensis* by much smaller body size, SVL 68.8 mm (vs. SVL 96.2 mm in female), fewer mid-ventral scale rows, MVSR 36 (vs. MVSR 40–42), fewer precloacal pores, PcP 10 (vs. 12 PcP in female); differs from *C. kiphire* **sp. nov.** by the number of paravertebral tubercles 32 (vs. PVT 26 or 29); differs from *C. lungleiensis* by fewer dorsal tubercle rows, DTR 17 (vs. 24–28), 10 precloacal pores (vs. 5–7 pitted precloacal scales in females); differs from *C. montanus* by fewer dorsal tubercle rows, DTR 17 (vs. DTR 21–23), fewer paravertebral tubercles, PVT 32 (vs. PVT 37–43), precloacal pores present (vs. PcP absent in female); differs from *C. myaleiktaung* by fewer mid-ventral scale rows, MVSR 36 (vs. MVSR 57), precloacal pores present (vs. PcP absent), broad regular dark bands absent on dorsum (vs. present); differs from *C. nagalandensis* by presence of 10 precloacal pores (vs. six pitted precloacal scales in female), 32 paravertebral tubercles (vs. PVT 35–37); differs from *C. namtiram* by fewer dorsal tubercle rows, DTR 17 (vs. DTR 21); differs from *C. ngopensis* by presence of 10 precloacal pores in female, (vs. 0–6 pitted precloacal scales in female); differs from *C. septentrionalis* by

fewer dorsal tubercle rows, DTR 17 (vs. DTR 23 or 24), less paravertebral tubercles, PVT 32 (vs. PVT 38–42), 10 precloacal pores present (vs. 14 precloacal scales with indistinct depression in female); differs from *C. siahaensis* by fewer dorsal tubercle rows, DTR 17 (vs. DTR 22–24), presence of precloacal pores in female (vs. PcP absent in female); differs from *C. vairengtensis* by the number of dorsal tubercle rows, DTR 17 (vs. DTR 22–23), 32 paravertebral tubercles (vs. PVT 34–39), 10 precloacal pores present (vs. 5–9 precloacal pits in female). Morphological differences with other members of *khasiensis* group is presented in Table 2.

Sequence divergence. *Cyrtodactylus barailensis* **sp. nov.** has a high genetic divergence of 10.9% from its closely related *C. namtiram*. With other members of the clade, *C. kiphirie* **sp. nov.** has a genetic divergence of 10.7% and 22.3% in the ND2 gene.

Etymology. The specific epithet is a toponym derived from the name of the hill range "Barail" where the type locality of the species lies.

Suggested common name. Barail Hills bent-toed gecko.

Distribution and natural history. During our two-day survey we only located a single individual of this species. Thus, the new species is currently known only from the type locality, in Peren District, Nagaland, India. We recorded this species on the trunk of a small tree at a height of approximately 2 m from the ground in the Athibung Reserve Forest at approximately 20:00 hrs on 14 August 2021. The forest type is semi-evergreen with relatively little anthropogenic pressure.

Cyrtodactylus manipurensis Boruah, Narayanan, Deepak & Das sp. nov.

https://zoobank.org/9AEE0E40-7983-444E-AC19-53AA8CE709D7

Figure 6; Tables 2, S2

Holotype. Adult male (WII-ADR1596), collected near Lamdan Kabui village (24.5954°N; 93.7085°E; elevation 1240 m a.s.l.) (Fig. 3A), Churachandpur District, Manipur, India collected by Bitupan Boruah on 25 July 2022.

Diagnosis. Medium-sized gecko, SVL at least 59.5 mm in adult male; 10 supralabials; eight or nine infralabials; 21 bluntly conical and feebly keeled tubercles across midbody; 37 paravertebral tubercles; 36 mid-ventral scales between ventrolateral folds; 11 or 12 subdigital lamellae beneath digit IV of manus; 13–16 subdigital lamellae beneath digit IV of pes; seven precloacal pores arranged in a continuous series; six irregular shaped dark-brown cross bands on back between axilla and groin; tail dorsally with eight dark-brown and seven pale-brown bands arranged alternatively.

Description of the holotype. Specimen well preserved except an incision below left axilla ventrolaterally. Snout-vent length 59.5 mm. Head moderately large (HL/SVL = 0.26), oval, dorsoventrally depressed, longer than width (HW/HL = 0.71), distinct from neck, broader at occipital region; snout tip rounded in both dorsal and lateral view; loreal region convex; canthus rostralis rounded, indistinct; interorbital space flat; a longitudinal furrow on dorsal surface of the snout; snout short (SO/HL = 0.39), longer than orbit (OD/SO = 0.68); nostril nearly rounded, opening directed posterolaterally; ear opening rounded; scales on head heterogeneous, largest on snout and loreal region, posteriorly smaller in upper eyelid, interorbital space and occipital region, granular juxtaposed; scales on upper eyelids heterogeneous; supraciliaries outwardly sharp giving serrated appearance in dorsal view, size anteriorly and posteriorly decreases, largest at the anterodorsal region; rostral wide, a short groove at the middle on top, rostral connected with nasals, supranasals, an internasal and first supralabials, two scales between the supranasals paced longitudinally, granular scales at parietal, occipital and temporal region intermixed with slightly large rounded granular tubercles starting from the level of posterior margin of the upper eyelids, those on temporal region are slightly larger than that of occipital region, size of the tubercles increases towards nape; 10 supralabial scales on both sides, size decreases towards angle of jaw; 8 supralabials up to midorbit on both sides; mental nearly triangular, connected with first infralabials, inner postmentals; nine infralabials on right side and eight on left side, size decreases towards angle of jaw; first infralabials connected with mental, second infralabial, inner and outer postmentals; inner pair of postmentals are larger than the outer postmentals; two rows of slightly enlarged scales along the infralabials starting below the outer postmentals, posteriorly size of those decreases; rest of the gular scales are small, granular juxtaposed, nearly homogeneous, size increases towards the throat where they become imbricate.

Habitus slender (BW/SVL = 0.16, TRL/SVL = 0.49), dorsoventrally depressed, dorsal scales granular, rounded, heterogeneous, intermixed with rounded, weakly keeled and bluntly conical tubercles irregularly arranged, up to third segment of the tail, size increases towards posterior body and pronounced at the base of tail; 21 dorsal tubercles across mid dorsum; 37 paravertebral tubercles; ventrolateral fold weak; ventral scales larger than those of dorsal, flat, smooth, cycloid subimbricate to imbricate; 36 mid-ventral scales between ventrolateral fold; seven precloacal pores arranged in an inverted "V" shaped continuous series, followed by a series of five unpored enlarged scales below it, largest at the apex, an unpored scale equal size to PcP present in continuous with the PcP in both ends; scales above the PcP larger than those of belly scales.

Forelimbs and hindlimbs slender (FL/SVL = 0.14, CL/SVL = 0.17), digits strongly inflected at the joints, all bearing large recurved claw, enlarged subdigital lamellae; lamellae beneath digit IV of right and left manus (given as basal + distal) is 6+5 and 6+6 respectively; lamellae be-

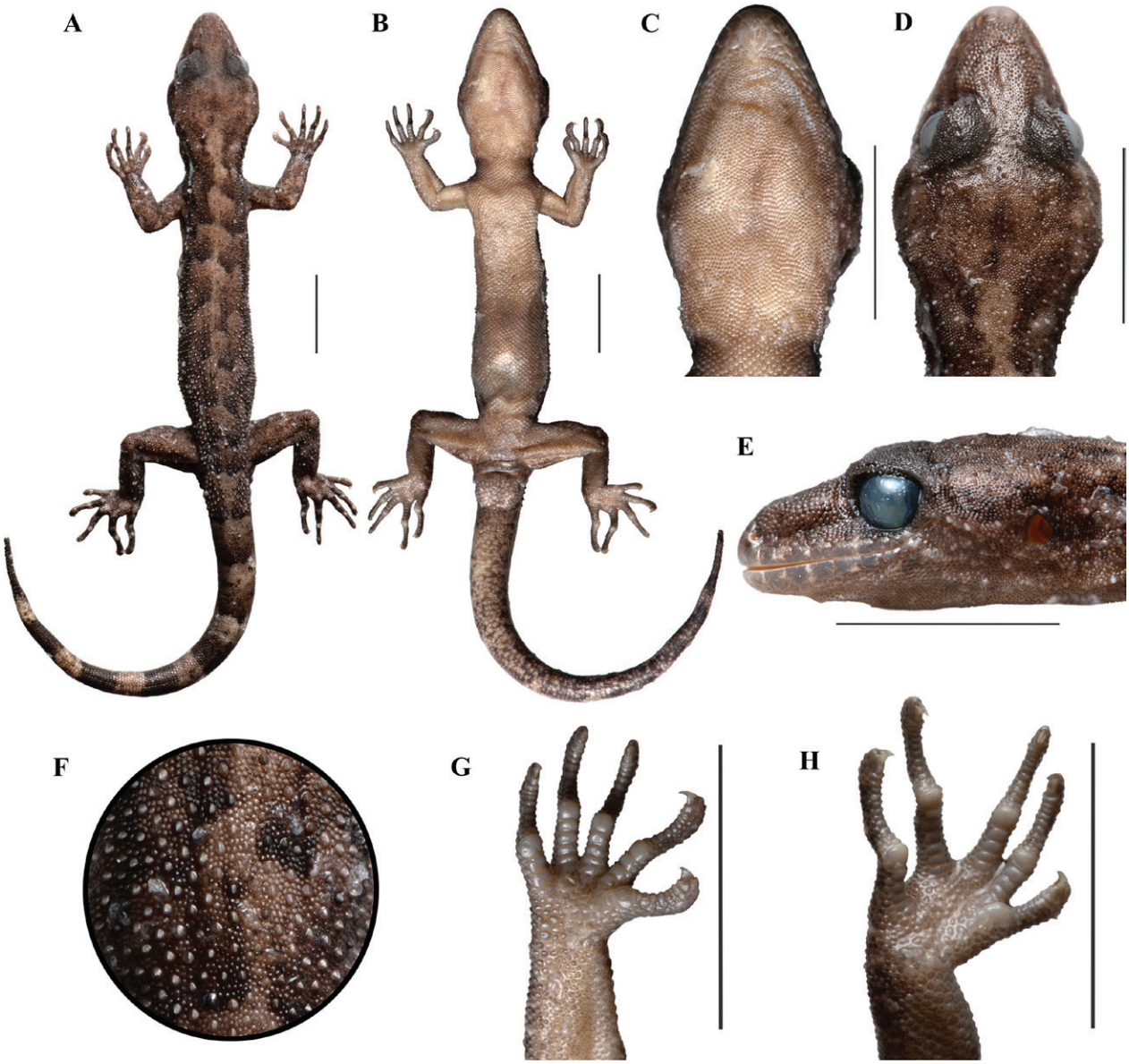

Figure 6. Holotype (WII-ADR1596) of *Cyrtodactylus manipurensis* **sp. nov.** in preserved condition. **A** dorsal and **B** ventral view of the whole body; **C** ventral, **D** dorsal, and **E** lateral view of head; **F** dorsal enlarged tubercles on trunk; **G** ventral view of right manus and **H** of right pes. Scale bar: 10 mm.

neath digit IV of both right and left pes (given as basal + distal) is 6+7 and 7+9 respectively; dorsal scales on forelimbs heterogeneous is size, mostly granular; proximal scales on upper arm are smaller than that of lower arm; scales near elbow on lower arm smooth and subimbricate; upper arm scales granular at proximal part and at the distal end it is smooth, cycloid and imbricate; dorsal scales of hindlimbs heterogeneous, intermixed with slightly enlarged, feebly keeled and bluntly conical tubercles; scales on inner lateral side of the thighs are smooth, large and subimbricate, those on dorsal side are small granular; scales on tibia are small, granular juxtaposed; ventral scales of forelimbs granular, juxtaposed, heterogeneous; scales on palm heterogeneous in shape and size, granular juxtaposed; ventral scales on hindlimbs heterogeneous; most of the thigh scales are smooth, cycloid and subimbricate, but on the knee and below the level of precloacal pores, scales are smaller and granular; scales above the vent granular; tibia scales smooth, nearly homogeneous, cycloid and subimbricate; scales on soles heterogeneous, granular, juxtaposed to subimbricate.

Tail complete (TL = 67 mm), slender, gradually tapering towards tip, segments indistinct, dorsal scales small, granular, juxtaposed at the base, posteriorly size increases, flat, smooth, subimbricate, heterogeneous in shape and size, large feebly keeled scales up to third segment of the tail, those on basal segment are pronounced; subcaudal scales smooth, subimbricate, wider than that of dorsal, heterogeneous in shape and size; no enlarged plate like series of subcaudal scales; three bluntly conical spurs on both sides of the tail base.

Colouration in preservative. Head on top and laterally brown; upper eyelids grey; dorsal ground colour of neck and back slightly paler than that of head; dark-brown irregular patches on neck up to fore limb insertion lev-

el; six irregular shaped dark-brown cross bands on back between axilla and groin, mid-dorsally interrupted; one dark-brown band on sacrum; tail dorsally with eight dark-brown and seven pale-brown bands arranged alternatively; dark bands are comparatively broader than the pale bands; the first dark-brown band on tail base broken mid-dorsally into two enlarged elongated spots. Ventrally head, neck, trunk and limbs light-brown; tail with irregular dark-brown specks.

Comparison. *Cyrtodactylus manipurensis* **sp. nov.** differs from *C. aaronbaueri* by fewer dorsal tubercle rows, DTR 21 (vs. DTR 22–28); differs from *C. aunglini* by fewer mid-ventral scale rows, MVSR 36 (vs. DTR 47–49), by fewer precloacal pores, PcP 7 (vs. PcP 12 or 13); differs from *C. barailensis* **sp. nov.** by number of dorsal tubercle rows, DTR 21 (vs. DTR 17), number of paravertebral tubercle rows, PVT 37 (vs. PVT 32); differs from *C. bengkhuaiai* by fewer dorsal tubercle rows, DTR 21 (vs. DTR 22–26); differs from *C. brevidactylus* by having fewer dorsal tubercle rows, DTR 21 (vs. DTR 27–30), enlarged chocolate-brown patches on head and back absent (vs. present); differs from *C. chrysopylos* by much smaller body size, SVL 59.5 mm (vs. SVL 64.9–79.1 mm in male), fewer precloacal pores, PcP 7 (vs PcP 8–13); differs from *C. dianxiensis* by smaller body size, SVL 59.5 mm (vs. SVL 73.8–79.9 mm), 21 rows of dorsal tubercle rows (vs. DTR 18 or 19); differs from *C. gansi* by fewer precloacal pores, PcP 7 (vs. PcP 16–29), ventrolateral fold present on trunk (vs. absent); differs from *C. jaintiaensis* by much smaller body size, SVL 59.5 mm (vs. SVL 87.0–88.3 mm in male), fewer precloacal pores in male, PcP 7 (vs. PcP 11 or 12); differs from *C. kiphire* **sp. nov.** by smaller body size, SVL 59.5 mm (SVL 63.9–64.7 mm), number of dorsal tubercle rows, DTR 21 (vs. DTR 16), number of paravertebral tubercle rows, PVT 37 (vs. PVT 26 or 29); differs from *C. lungleiensis* by higher number of precloacal pores, PcP 7 (vs. PcP 3–5 in male), fewer dorsal tubercle rows, DTR 21 (vs. 24–28); differs from *C. montanus* by larger body size, SVL 59.5 mm (vs. 53.6–55.0 mm in male); differs from *C. myaleiktaung* by fewer mid-ventral scale rows, MVSR 36 (vs. MVSR 57), precloacal pores present (vs. PcP absent), broad regular dark bands absent on dorsum (vs. present); differs from *C. nagalandensis* by higher number of dorsal tubercle rows, DTR 21 (vs. DTR 16–18); differs from *C. namtiram* by having fewer precloacal pores, PcP 7 (vs. PcP 12); differs from *C. ngopensis* by the number of precloacal pores, PcP 7 (vs. PcP 6); differs from *C. siahaensis* by be fewer subdigital lamellae, 11 or 12 lamellae under fourth finger (vs. 13 or 14 lamellae under fourth finger), dark-brown broad bands consists of two series of enlarged spots on dorsum (vs. dark-brown blotches in the form of reticulation on dorsum); differs from *C. vairengtensis* by fewer precloacal pores, PcP 7 (vs. PcP 9–11). Morphological differences with other members of *khasiensis* group is presented in Table 2.

Sequence divergence. *Cyrtodactylus manipurensis* **sp. nov.** has a high genetic divergence of 11.2–11.3% from its closely related *C. ngopensis*, 10–10.3% from *C. aaronbaueri*, 10.2–10.5% from *C. vairengtensis* and 9.7–11.1% from the *C. montanus*. With other members of the clade, *C. kiphirie* **sp. nov.** has a genetic divergence of 8.6% and 23% in the ND2 gene.

Etymology. This species is named after Manipur state in India.

Suggested common name. Manipur bent-toed gecko.

Distribution and natural history. *Cyrtodactylus manipurensis* **sp. nov.** is currently only recorded from the type locality. We collected a single individual at 18:00 hrs on 25 July 2022 near Lamdan Kabui village. It was perched on a shrub at a height of approximately 1.5 m, on the road connecting Leimatak and Charoikhullen. The habitat is secondary forest, with *Zingiber* sp. cultivation and settlements.

khasiensis clade

This clade was strongly supported in both analyses (UFB 100, PP 1.0) and clustered with poor support (UFB 73, PP 0.79) as sister to the *gansi* clade comprising 11 described species and one undescribed lineage. The samples from Ngengpui Wildlife Sanctuary (Mizoram) included in this study were recovered with strong support in both ML and BI (UFB 99, PP 1) as sister to *C. ayeyarwadyensis*. This lineage was recovered as a distinct species unit in all of our species delimitation analyses (Fig. 2) and is described below.

Diagnosis. Members of the *khasiensis* clade can distinguished by the following set of morphological characters: SVL 48.1–80.0 mm in adult males and SVL 57.5–81.1 mm in adult females; 8–13 supralabials and 8–11 infralabials; 18–25 rows of tubercles across mid-dorsum; 29–40 paravertebral tubercles between the level of axilla and groin; 30–43 mid-ventral scales; 9–28 precloacal pores or 26–39 precloacofemoral pores in males; precloacal pores in females may be absent, or 11–14 pitted scales or 10–16 small precloacal pores present; ventrolateral skin fold present; 11–23 subdigital lamellae on fourth finger; 12–27 subdigital lamellae on fourth toe; enlarged plate-like subcaudal scales absent except in *C. khasiensis*.

Cyrtodactylus ngengpuiensis Boruah, Narayanan, Lalronunga, Deepak & Das sp. nov.

https://zoobank.org/D04AF555-89A2-467F-B5CE-419328F6934F

Figure 7; Tables 2, S2

Holotype. Adult male (WII-ADR1057; Fig. 7A–J), from Ngengpui Wildlife Sanctuary (22.4906°N; 92.7575°E; elevation 160 m a.s.l.) (Fig. 3A), Lawngtlai District,

Mizoram, India collected by Abhijit Das, Bitupan Boruah and Samuel Lalronunga on 8 September 2021.

Paratypes. Two adult females (WII-ADR991 and WII-ADR1058) and one subadult female (WII-ADR1059) collected from the same locality in Ngengpui Wildlife Sanctuary by the same team on 7 and 8 September 2021.

Diagnosis. Medium-sized gecko (SVL at least 61.2 mm in adult male and 72–74.1 mm in adult females); 9–12 supralabials; 8–11 infralabials; 18–20 bluntly conical and feebly keeled dorsal tubercles; 29–34 paravertebral tubercles; 38 or 39 midventral scale rows between the weak ventrolateral folds; no precloacal groove; at least 27 precloacofemoral pores in continuous series in male and 10–16 small precloacal pores in females; short dark-brown bars between a pair of dorsolateral stripes or enlarged irregular dark-brown spots present on dorsum.

Description of holotype. Holotype well preserved except an incision below left axilla ventrolaterally. Snout-vent length 61.2 mm. Head moderately large (HL/SVL = 0.27), dorsoventrally depressed, longer than width (HW/HL = 0.68), distinct from neck, broader at occipital region, snout tip rounded in both dorsal and lateral view, loreal region convex, canthus rostralis rounded, indistinct, interorbital space flat, a longitudinal furrow on dorsal surface of the snout, snout short (SO/HL = 0.4), longer than orbit (OD/SO = 0.66), nostril nearly rounded, opening directed posterolaterally, ear opening oval and oblique, scales on head heterogeneous, largest on snout and loreal region, posteriorly smaller in upper eyelid, interorbital space and occipital region, granular juxtaposed, scales on upper eyelids heterogeneous, supraciliaries outwardly sharp giving serrated appearance in dorsal view, size anterior and posterior end decreases, rostral wide, a short groove at the middle on top, rostral connected with nasals, supranasals, an internasal and first supralabials, two scales between the supranasals, larger than the rest of the granular snout scales, granular scales at parietal region and occipital region intermixed with slightly large rounded granular tubercles, dense in occipital and temporal region and size increases towards nape, nine supralabials on right and 10 on left side, size decreases towards angle of jaw, supralabials up to midorbit seven on right and eight on left side, a series of narrow and slightly elongated scales above the supralabials between nostril and anterior border of the orbit, mental as wide as rostral, triangular, connected with first infralabials, inner postmentals, nine infralabials on both side, size decreases towards angle of jaw, first infralabials connected with mental, second infralabial, inner and outer postmentals, inner pair of postmentals are larger than the outer postmentals, posterior margin of the inner postmentals bordered by seven granular scales of different size, two or three rows of enlarged scales along the infralabials starting below the outer postmentals, posteriorly size of those decreases, elongated and narrow, rest of the gular scales are small, granular juxtaposed, homogeneous, size increases towards the throat where they become imbricate.

Habitus slender (BW/SVL = 0.17, TRL/SVL = 0.41), dorsoventrally depressed, dorsal scales granular, rounded, heterogeneous, intermixed with rounded, weakly keeled and bluntly conical tubercles irregularly arranged, starting from occipital region to seventh segment of the tail, size increases towards posterior body, pronounced at sacrum and base of the tail, 18 dorsal tubercles across mid dorsum, 29 paravertebral tubercles, ventrolateral fold weak, ventral scales larger than those of dorsal, flat, smooth, cycloid subimbricate to imbricate, largest on belly, 39 mid-ventral scales between ventrolateral fold, 27 precloacal femoral (PcFP) pores in a continuous series (Fig. 7I), followed by eight unpored, large scales below the PcFP at the middle.

Forelimbs and hindlimbs slender (FL/SVL = 0.14, CL/SVL = 0.19); digits strongly inflected at the joints, all bearing large recurved claw, enlarged subdigital lamellae; lamellae beneath digit IV of right and left manus (given as basal + distal) is 5+8 and 5+9 respectively; lamellae beneath digit IV of right and left pes (given as basal + distal) is 4+10 and 5+10 respectively; dorsal scales on forelimbs heterogeneous, granular juxtaposed; dorsal scales of hindlimbs heterogeneous, granular, intermixed with densely placed large, rounded and bluntly conical tubercles, scales on inner lateral side of the thighs near knee are subimbricate; ventral scales of forelimbs granular, juxtaposed, mostly homogeneous; scales on palm heterogeneous in shape and size, granular; scales on ventral side of hindlimbs nearly equal to those of belly, smooth, cycloid and subimbricate, but on the knee, above cloaca and on thigh below the level of precloacal pores are smaller and granular; scales on soles heterogeneous, granular, juxtaposed to subimbricate.

Tail complete (TL = 70 mm), slender, gradually tapering towards tip, segments indistinct, dorsal scales granular, juxtaposed, flat, smooth, heterogeneous in shape and size; enlarged feebly keeled scales up to eight segments of the tail, those on basal segment are pronounced; subcaudal scales smooth, subimbricate, wider than that of dorsal, heterogeneous in shape and size; no enlarged plate like series of subcaudal scales.

Colouration in life. Fig. 7J. Top of head pale-brown with indistinct pale-cream coloured spots on anterior part, a few slightly dark-brown patches on upper eyelids, temporal and occipital region; supraciliary yellowish-brown; dark-brown postocular streak on each side which continues dorsolaterally along neck and trunk to tail base, on right side this stripe is disjunct; a pale-cream coloured steak on each side of the dark-brown post orbital streak; an indistinct brown stripe along loreal region and a pale-cream coloured streak above it; upper lip with irregular brown and pale-yellow spots; a pair of dark-brown stripe with irregular edge on neck interspaced by an elongated pale-cream coloured patch, posterior ends of these stripes are connected; an enlarged dark-brown spot at the middle of nape; a pair of narrow pale-cream coloured stripe on neck above the lateral dark-brown stripe running up to slightly behind the level of axilla; dorsum pale-brown with seven irregular shaped and sized, broad dark-brown

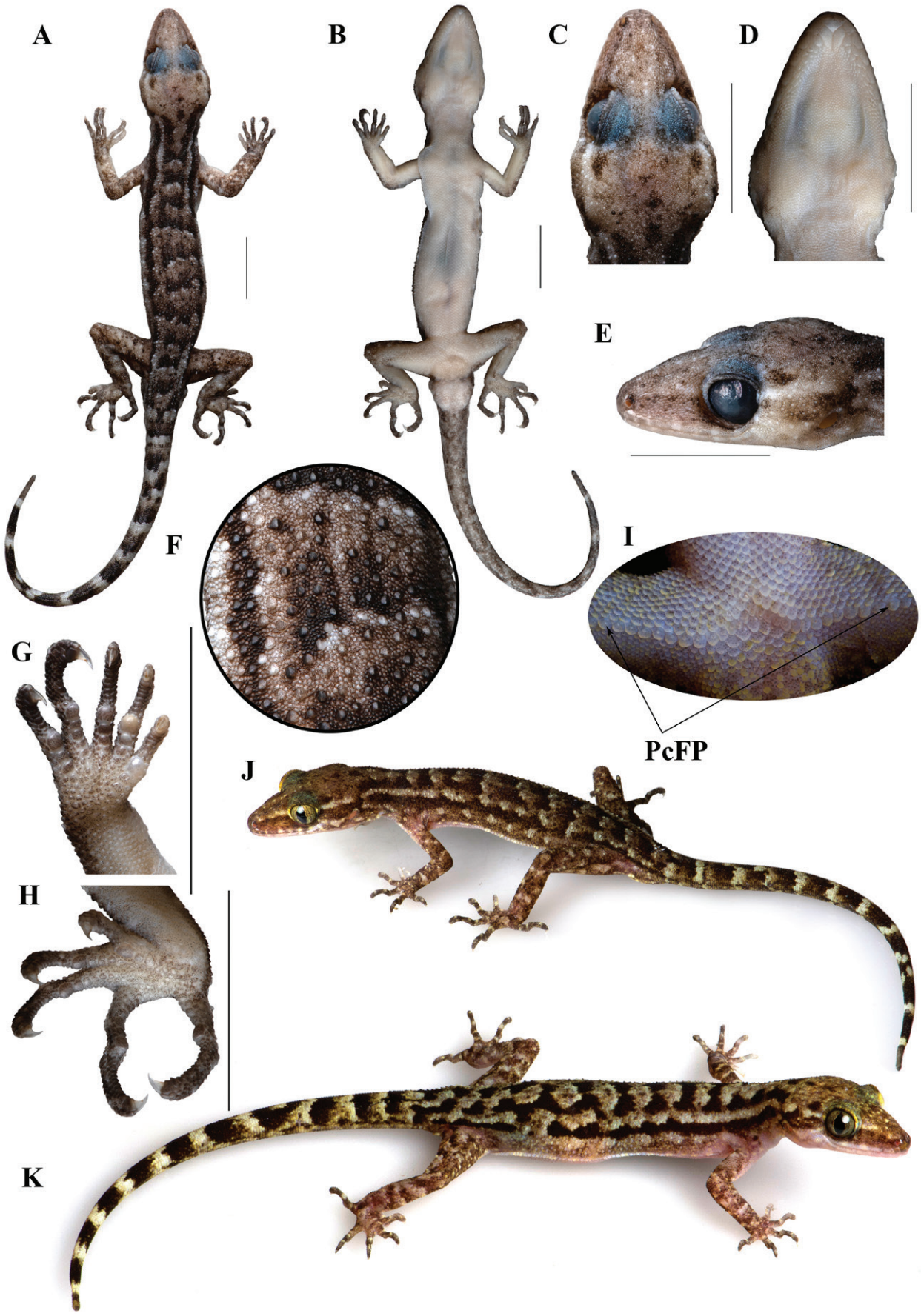

Figure 7. *Cyrtodactylus ngengpuiensis* **sp. nov**. **A**–**J** holotype (ADR-WII1057), **A** dorsal and **B** ventral view of the whole body; **C** dorsal, **D** ventral, and **E** lateral view of head; **F** dorsal tubercles on trunk; **G** ventral view of right manus, and **H** right pes, **I** precloacofemoral pores; **J** holotype (ADR-WII1057), and **K** paratype (WII-ADR991) in life. Scale bar: 10 mm. **J, K** not to scale.

cross bars, these bars posteriorly edged with narrow cream coloured patch, first two cross bars are shorter than the rests; a few enlarged whitish spots along lateral side of the trunk; dorsally limbs pale-brown intermixed with slightly darker spots and light patches; dorsally tail with alternating slightly dark-brown broad bands and narrow pale-cream coloured bands of irregular shape and size; spurs cream coloured; ventrally head and trunk whitish with pinkish tinge and scales with brown marbling; some scales above and below the cloaca are pale-yellow; tail with slightly dense brown marbling.

Colouration in preservative. Dorsal and ventral colour nearly the same as that of in life; dorsal markings visible as that of life condition.

Morphological variation. Details of the variations in morphometric and meristic characters of the type series are provided in Table S2. Apart from these dorsal markings among the paratypes slightly varied. In the two paratypes (WII-ADR1058 and WII-ADR1059), dorsal bands are broken mid dorsally giving the appearance of enlarged spots (Fig. S2). Precloacal pores in female are smaller than that of male.

Comparison. *Cyrtodactylus ngengpuiensis* **sp. nov.** can be differentiated from the members of the *C. khasiensis* clade (except *C. ayeyarwadyensis*, *C. guwahatiensis*, *C. karsticola* and *C. tripuraensis*) by the presence of precloacofemoral pores in male (vs. no femoral pores in male of *C. agarwali*, *C. exercitus*, *C. kazirangaensis*, *C. khasiensis*, *C. septentrionalis*, *C. urbanus*). *Cyrtodactylus ngengpuiensis* **sp. nov.** differs from *C. ayeyarwadyensis* by presence of tiny precloacal pores in female, PcP 10–16 (vs. PcP absent in female); differs from *C. bapme* by presence of 10–16 precloacal pores in female (vs. 0–13 pitted precloacal scales), dorsal tubercle rows, DTR 18 or 20 (vs. 21–24); differs from *C. guwahatiensis* by fewer preclocaofemoral pores, PcFP 27 (vs. PcFP 35–39), PcFP in a continuous series (vs. 26 PcFP interrupted by 11 unpored scales in holotype *C. guwahatiensis*), PcP present in females (vs. PcP absent in females), higher mid-ventral scale rows, MVSR 38–39 (MVSR vs. 30–35), fewer dorsal tubercle rows, DTR 18–20 (vs. DTR 21–24); differs from *C. karsticola* by fewer precloacal femoral pores in male, PcFP 27 (vs. PcFP 34–38), less number of dorsal tubercle rows, DTR 18–20 (vs. DTR 21–24), fewer paravertebral tubercles, PVT 29–34 (vs. PVT 34–39); differs from *C. tripuraensis* by fewer precloacal femoral pores in male, PcFP 27 (vs. PcFP 29–37) and less number of precloacal pores, PcP 10–16 in female (vs. PcP 19–29 in female). Morphological differences with other members of *khasiensis* group is presented in Table 2.

Sequence divergence. *Cyrtodactylus ngengpuiensis* **sp. nov.** has a moderate genetic divergence of 4.1–6.6% from its closely related *C. ayeyarwadyensis*, 4.2–6.0% from *C. tripuraensis*. With other members of the clade, *C. ngengpuiensis* **sp. nov.** has a genetic divergence between 8.6% and 15.7% in the ND2 gene. The intraspecific divergence is between the two samples of *C. ngengpuiensis* **sp. nov.** is 0.8%.

Etymology. The specific epithet is a toponym derived from the name "Ngengpui Wildlife Sanctuary" of Mizoram state from where the type series of the species were collected.

Suggested common name. Ngengpui bent-toed gecko.

Distribution and natural history. *Cyrtodactylus ngengpuiensis* **sp. nov.** new species is currently only known from the type locality, the Ngengpui Wildlife Sanctuary, Lawngtlai District, Mizoram, India. The forest is characterised as tropical semi-evergreen to moist evergreen forest. The forest is dominated by *Dipterocarpus* spp., palms, canes and rattans. Individuals of *C. ngengpuiensis* **sp. nov.** were collected during 6–9 September 2021 at 21:00–22:00 hrs. Individuals were recorded in bamboo thickets, on tree buttresses and trunks, and amongst ferns and rocks along the banks of evergreen forest streams.

mombergi clade

This monophyletic clade was well-supported in both analyses (UFB 100, PP 1.0) and is most closely related to the sister clades *gansi* and *khasiensis*. The *mombergi* clade comprises one described species and two additional undescribed lineages, *C.* cf. *mombergi* and another lineage described below as a new species (Fig. 2). Eight samples from Namdapha Tiger Reserve, samples from Kamlang Tiger Reserve and Hornbill of Namdapha Tiger Reserve (Arunachal Pradesh), and two samples (CES13/1459, CES11/1349) from GenBank (Miao, Arunachal Pradesh) were found monophyletic with both ML and weak support in BI analyses (UFB 95, PP 0.76) and correspond to the species described below. In the phylogenetic analyses, it was sister to a clade containing *C. mombergi* and *C.* cf. *mombergi*.

Diagnosis. Members of the *mombergi* clade can be distinguished by the following set of morphological characters: SVL 57.5–70.7 mm in adult males and SVL 54.8–74 mm in adult females; 8–11 supralabials and infralabials; 11–22 subdigital lamellae on fourth toe; 17–27 rows of tubercles across mid-dorsum; 29–42 paravertebral tubercles between the level of axilla and groin; 31–40 mid-ventral scales; 7–11 precloacal pores in males; 8–10 precloacal pores in females or it may be absent; ventrolateral skin fold on trunk present.

Cyrtodactylus namdaphaensis Boruah, Narayanan, Deepak & Das sp. nov.

https://zoobank.org/C45008F3-D9E2-473A-B72A-DE92D00C73E4

Figure 8; Tables 2, S2

Holotype. Adult male (WII-ADR1416), collected from Kamala Valley (27.4595°N; 96.4279°E; elevation 650 m a.s.l.), Namdapha Tiger Reserve, Changlang District, Arunachal Pradesh, India by Abhijit Das and Bitupan Boruah on 18 May 2022 (Fig. 3A).

Paratypes. Two adult males (WII-ADR1415, WII-ADR1417) collected from the same locality as the holotype on the same date; one adult female (WII-ADR1404) collected near Deban (27.4942°N; 96.3701°E; elevation 400 m a.s.l.), Namdapha Tiger Reserve, Changlang District, Arunachal Pradesh, India by Abhijit Das and Bitupan Boruah on 11 May 2022; two adult females (WII-ADR3067, WII-ADR3068) collected from Motijheel trail (27.4899°N, 96.3348°E; elevation 470 m a.s.l.), Gibbons' Land, Namdapha Tiger Reserve, Changlang District, Arunachal Pradesh, India by Abhijit Das and Bitupan Boruah on 11 September 2022; one adult female (WII-ADR1790) collected near Burma Nullah (40 mile point) (27.4878°N; 96.5416°E; elevation 480 m a.s.l.), Namdapha Tiger Reserve, Changlang District, Arunachal Pradesh, India by Abhijit Das and Bitupan Boruah on 18 September 2022.

Referred materials. An adult female (WII-ADR3060) collected from Sinabrai (27.7434°N; 96.3872°E; elevation 470 m a.s.l.), Kamlang Tiger Reserve, Lohit District, Arunachal Pradesh, India on 5 September 2022 by Bitupan Boruah and Abhijit Das; an adult female (WII-ADR3281) and an adult male (WII-ADR3282) collected from Hornbill (27.5381°N; 96.4403°E; elevation 670 m a.s.l.), Namdapha Tiger Reserve, Changlang District, Arunachal Pradesh, India on 10 May 2023 by Rajiv N.V.

Diagnosis. Medium-sized gecko (SVL 57.5–70.7 mm in males and SVL 54.8–69.3 mm in females); supralabials and infralabials 8–11; dorsum with weakly keeled and bluntly conical tubercles, 29–36 paravertebral tubercles between the level of axilla and level of groin; 17–19 dorsal tubercle rows at mid body; 33–40 mid ventral scale rows; seven to nine precloacal pores in males and 8–10 small precloacal pores in females in a continuous series, PcP much smaller in females than that of males; 12–14 subdigital lamellae on finger IV and 11–17 subdigital lamellae on toe IV; irregular dark-brown spots or stripes on dorsum.

Description of holotype. Holotype well preserved except a ventrolateral incision below left axilla. Snout-vent length 65.3 mm. Head moderately large (HL/SVL = 0.27), dorsoventrally depressed, ovoid in shape, longer than width (HW/HL = 0.66), distinct from neck, broader at occipital region; snout rounded in both dorsal and lateral view; loreal region convex; canthus rostralis rounded, indistinct; interorbital space flat, a longitudinal furrow on dorsal surface of the snout, snout short (SO/HL = 0.4), longer than orbit (OD/SO = 0.71); nostril semicircular, opening directed posterolaterally; ear opening oval and oblique; scales on head heterogeneous, largest on snout and loreal region, posteriorly smaller, interorbital space and occipital region, granular juxtaposed; scales on upper eyelids nearly homogeneous, granular juxtaposed; supraciliaries outwardly sharp giving serrated appearance in dorsal view, size anteriorly and posteriorly decreases, largest at the anterodorsal region; rostral wide, a short groove at the middle on top, rostral connected with nasals, supranasals, internasals and first supralabials; granular scales at parietal, occipital and temporal region intermixed with slightly large, rounded and bluntly conical tubercles, dense in occipital and temporal region and size increases towards nape; supralabial 11 on right and 10 on left side, supralabials up to midorbit eight on right and seven on left side, size decreases towards angle of jaw; a series of scales slightly larger than the loreal scales present above the supralabials, posteriorly size decreased; mental as wide as rostral, nearly triangular, connected with first infralabials, inner postmentals; nine infralabials on right and eight on left side, size decreases towards angle of jaw; inner pair of postmentals are larger than the outer postmentals; two rows of enlarged scales along the infralabials starting below the outer postmentals, posteriorly size of those decreases; rest of the gular scales are small, granular juxtaposed, homogeneous, size increases towards throat where they becomes imbricate.

Habitus slender (BW/SVL = 0.17, TRL/SVL = 0.47), dorsoventrally depressed; dorsal scales granular, rounded, heterogeneous, intermixed with rounded, irregularly arranged weakly keeled and bluntly conical tubercles, these tubercles continues to fourth segment of the tail, size increases towards posterior body and pronounced; 18 dorsal tubercles across mid dorsum; 36 paravertebral tubercles; ventrolateral fold weak; ventral scales larger than those of dorsal, flat, smooth, cycloid subimbricate to imbricate, largest towards belly; 40 mid-ventral scales between ventrolateral fold; seven precloacal pores arranged in an inverted "V" shaped continuous series, followed by five unpored, large scales below it, one enlarged unpored scale present on right end of the PcP series.

Forelimbs and hindlimbs slender (FL/SVL = 0.15, CL/SVL = 0.18); digits strongly inflected at the joints, all bearing large recurved claw, enlarged subdigital lamellae; lamellae beneath digit IV of right and left manus (given as basal + distal) is 5+8; lamellae beneath digit IV of right and left pes (given as basal + distal) is 6+8 and 5+8 respectively; dorsal scales on forelimbs smooth, subimbricate and heterogeneous, small and granular at elbow, scales on forearm nearly rounded while those on hind arm are posteriorly tapering; forearm scales intermixed with enlarged rounded and bluntly conical tubercles; dorsal scales of hindlimbs heterogeneous, intermixed with large, rounded and bluntly conical tubercles, dense than those on forelimbs; horizontally upper half of the thigh scales are smooth, large and subimbricate, those on lower half small granular; scales on tibia are small, granular juxtaposed; ventral scales of forelimbs granular, juxtaposed, mostly homogeneous; scales on palm heterogeneous in shape and size, granular juxtaposed; scales on ventral side of hindlimbs smaller than those of belly, smooth, cycloid and subimbricate, but on the knee, above cloaca and on thigh below the level of precloacal pores are smaller

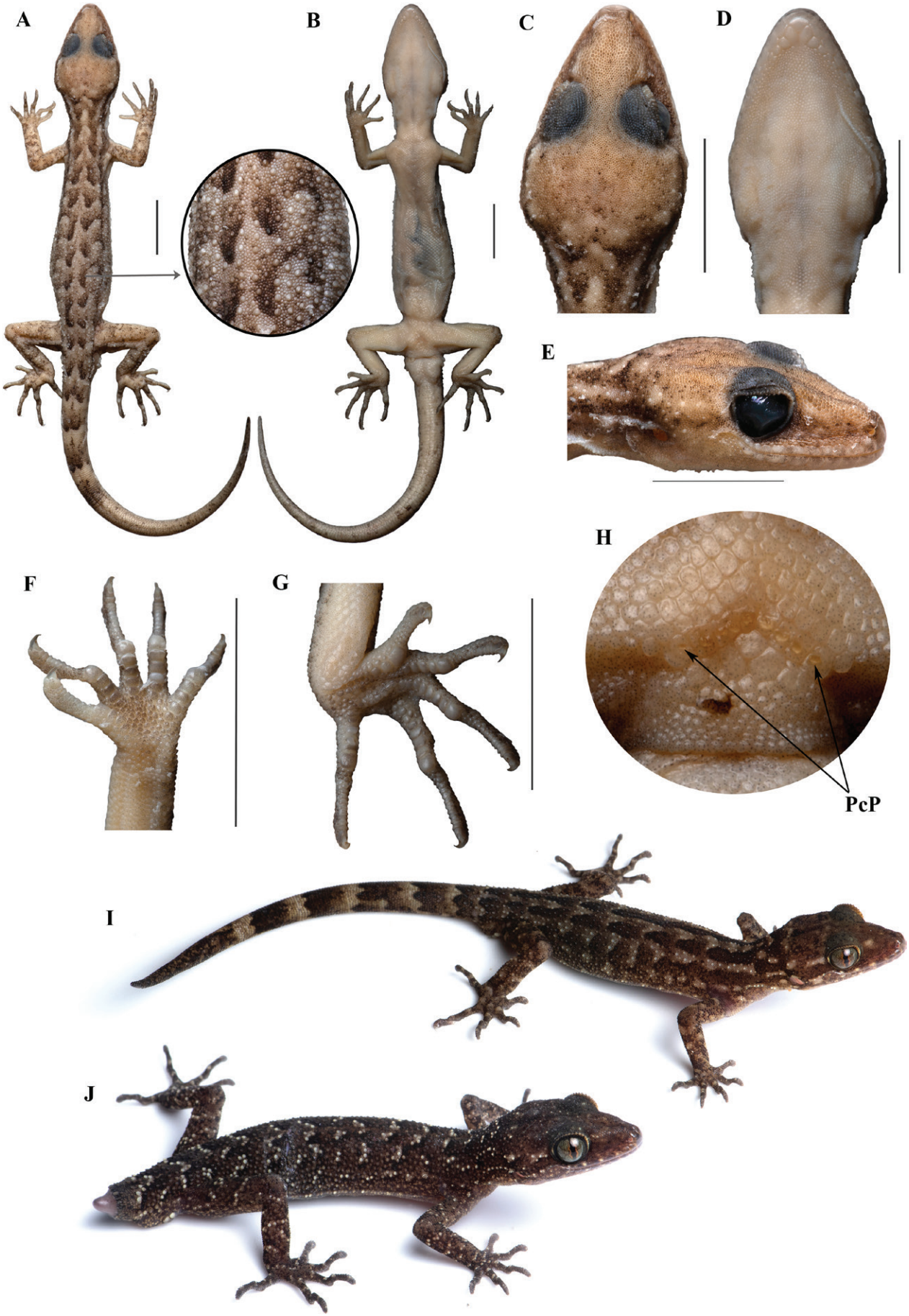

Figure 8. *Cyrtodactylus namdaphaensis* **sp. nov. A**–**G** holotype (WII-ADR1416), **A** dorsal, and **B** ventral view of the whole body; **C** dorsal, **D** ventral, and **E** lateral view of head; **F** ventral view of left manus and **G** left pes; **H** precloacal pores of paratype WII-ADR1417; **I** paratype WII-ADR1417, and **J** paratype WII-ADR1415 in life. Scale bar: 10 mm. **I, J** not to scale.

and granular; scales on soles heterogeneous, granular, juxtaposed to subimbricate.

Tail regenerated (TL = 79 mm), slender, gradually tapering towards tip, segments indistinct, in the original part of the tail dorsal scales small, granular, juxtaposed at the base, posteriorly size increases, flat, smooth, subimbricate, heterogeneous in shape and size; in the regenerated part of the tail, scales are irregular in shape and size; large feebly keeled scales upto fourth segment of the tail, those on basal segment are pronounced; subcaudal scales smooth, subimbricate, wider than that of dorsal, heterogeneous in shape and size; no enlarged plate like series of subcaudal scales; two and four bluntly conical spurs on right and left side of the tail base respectively.

Colouration in preservative. Top of head pale-brown, upper eyelids grey; neck and dorsum dorsally greyish-brown; two brown stripes with irregular edge on dorsal side of the neck continuing to the level of forelimb insertion, and another stripe on each lateral side of the neck; seven pairs of slightly dark-brown elongated spots of irregular shape and size on dorsum, these spots are outwardly connected to a narrow, brown dorsolateral stripe; tail dorsally pale-brown with broad dark-brown cross bars of irregular shape and size on the original part, the first bar broken into two elongated spots, regenerated part of the tail is plain pale-brown; ventrally head, trunk and tail pale-cream coloured, a few irregular brown spots on tail.

Colouration in life. (Based on paratype WII-ADR1417) (Fig. 8I); head dorsally brown with irregular dark-brown patches, a pair of pale-yellowish spots on loreal in front of anterodorsal corner of eyes, lips slightly paler than dorsal head colour with irregular pale-yellowish spots; a pale-brown postorbital streak; pale-brown irregular spots on dark-brown background on neck; upper eyelids greyish-brown; slightly dark-brown large spots of irregular size and shape on dorsal and lateral side of the trunk, interspaced with pale-brown patches, dark-brown spots on dorsal side of the trunk giving appearance of continuous stripes up to middle of the trunk; anterior two third of dorsal side of the tail with alternative broad dark-brown and narrow pale-brown bands, those dark-brown bands anteriorly diffused and posterior edge zigzagged, posterior one third brown with dark-brown marbling; limbs brown with irregular pale spots and dark-brown reticulation; digits with alternative dark-brown and pale-brown bands.

Morphological variation. Morphological variations are given in Table S2. Except for those, the dorsal marking pattern varied among the collected specimens. The dorsal spots of WII-ADR1417 are in the form of two continuous stripes starting from neck, posteriorly broken; a spot at the middle of occipital region followed by a dark cross bar on the nape; WII-ADR3067 and WII-ADR3281 has four dorsal stripes starting from neck to the level of hind limb insertion; WII-ADR3068 has four stripes on neck, followed by five irregular and zigzag cross bars on dorsum; in WII-ADR1790, dorsal spots are indistinct and irregular; WII-ADR1415 has three pairs of dark spots posteriorly bordered with white spots on neck, cross bars on dorsum narrower, irregular and posteriorly with white (Fig. S2); WII-ADR3060 has six dark brown cross bands on back between the level of axilla and groin, consists of irregular shaped enlarged individual spots, mid dorsally these spots are remarkably disjunct,. Precloacal pores in females are smaller than that of males.

Comparison. *Cyrtodactylus namdaphaensis* **sp. nov.** differs from *C. mombergi* by fewer dorsal tubercle rows, DTR 17–19 (vs. DTR 23–27), by fewer precloacal pores, PcP 7–9 (vs. PcP 10–11). Morphological differences with other members of *khasiensis* group is presented in Table 2.

Sequence divergence. *Cyrtodactylus namdaphaensis* **sp. nov.** has a moderate genetic divergence of 6.2–7.9% from the closely related *C. mombergi*. The intraspecific divergence among the thirteen samples of *C. namdaphaensis* **sp. nov.** ranges between 0.1–5%.

Etymology. The specific epithet is a toponym named after its type locality Namdapha Tiger Reserve in Arunachal Pradesh, India.

Suggested common name. Namdapha bent-toed gecko.

Distribution and natural history. So far, *Cyrtodactylus namdaphaensis* **sp. nov.** has been recorded within an elevational range of 400–650 m a.s.l. inside Namdapha Tiger Reserve. All the localities are south of Noa-Dihing River in Changlang District, Arunachal Pradesh, India. We recorded this species between May and September 2022. Individuals were recorded on tree bark, ferns, and riparian vegetation and along forest trails between 18:00–23:00 hrs. The forest type can be classified as Assam Valley Tropical Evergreen Forest. The area had a distinct understory with a thick covering of leaf-litter. Currently the species has been recorded from 25 Mile, Burma Nullah (40 Mile), Gibbons Land, Motijheel trail and at Hornbill camp located at the north bank of Noa-Dihing River within the Namdapha Tiger Reserve. We also recorded this species on rocks and vegetation near Kamlang River at Sinabrai, near the Kamlang Tiger Reserve, at an elevation of 470 m a.s.l. We observed juveniles of this species on the forest floor in the leaf litter during May, 2022. During 2023, adult individuals were seen on the ferns overhanging first order streams. At the slightest disturbance, the lizards would drop into the thick vegetation below. Other arboreal reptile taxa from the area included *Ptyctolaemus* sp., *Japalura* sp. and *Pareas* sp.

cayuensis clade

Diagnosis. Members of the *cayuensis* clade can be diagnosed by the following set of morphological characters: SVL 61.2–83.5 mm in adult males and SVL 59.4–83.6 mm in adult females; 8–13 supralabials and 8–12 infralabials; 15–26 rows of tubercles across mid-dorsum; 26–38 para-

vertebral tubercles between the level of axilla and groin; 28–45 mid-ventral scales; 13–21 subdigital lamellae on fourth finger; 11–23 subdigital lamellae on fourth toe; 6–10 precloacal pores in males; 7–10 small precloacal pores in females; ventrolateral skin fold on trunk present.

Cyrtodactylus siangensis Boruah, Narayanan, Aravind, Deepak & Das sp. nov.

https://zoobank.org/B53EA935-E7F2-480B-8771-240B3A6E9939

Figure 9; Tables 2, S2

Holotype. Adult female (WII-ADR1177; Fig. 9A, B, E–I), from Kalek stream (28.1711°N; 95.2420°E, elevation 210 m a.s.l.; Fig. 3A); 1.8 km (aerial distance) northwest from Bodak village, East Siang District, Arunachal Pradesh, India collected by Bitupan Boruah on 23 October 2021.

Paratypes. Two adult females (WII-ADR1581 and WII-ADR1582; Fig. 9C, D) from a hill slope near Kalek stream, East Siang District, Arunachal Pradesh, India collected by Bitupan Boruah on 15 June 2022.

Diagnosis. Medium-sized gecko (SVL 70.1–72.1 mm in females); males unknown; supralabials 8–12 and infralabials 9–12; tubercles on dorsum weakly keeled and bluntly conical, 26–32 paravertebral tubercles between the level of axilla and level of groin; 15 or 16 dorsal tubercle rows at mid body; 40–45 mid ventral scale rows; 8–10 small precloacal pores in a continuous series; 13–17 subdigital lamellae on finger IV and 14–19 subdigital lamellae on toe IV; six or seven irregular and broken dark-brown bands on dorsum between the level of axilla and level of groin, or irregular dark-brown reticulation on dorsum.

Description of the holotype. Holotype well preserved except an incision below left axilla ventrolaterally. Snout-vent length 72.1 mm. Head moderately large (HL/SVL = 0.26), dorsoventrally depressed, longer than width (HW/HL = 0.72), distinct from neck, broader at occipital region; snout rounded in both dorsal and lateral view; loreal region convex; canthus rostralis rounded, indistinct; interorbital space flat, a longitudinal furrow on dorsal surface of the snout, snout short (SO/HL = 0.39), longer than orbit (OD/SO = 0.73); nostril nearly rounded, opening directed posterolaterally; ear opening oval and oblique; scales on head heterogeneous, largest on snout and loreal region, posteriorly smaller in upper eyelid, interorbital space and occipital region, granular juxtaposed; scales on upper eyelids heterogeneous; supraciliaries outwardly sharp giving serrated appearance in dorsal view, size anteriorly and posteriorly decreases, largest at approximately anterior one third of it; rostral wide, a short groove at the middle on top, rostral connected with nasals, supranasals, an internasal and first supralabials; a single scale between the supranasals, larger than the rest of the granular snout scales; granular scales at parietal region and occipital region intermixed with slightly large rounded granular tubercles, dense in occipital and temporal region and size increases towards nape; supralabial eight on right and 11 on left side, supralabials upto midorbit seven on right and eight on left side, size decreases towards angle of jaw; a series of scales nearly rounded, granular and slightly larger than the loreal scales present above the supralabials; mental as wide as rostral, triangular, connected with first infralabials, inner postmentals; 10 infralabials on right and nine on left side, size decreases towards angle of jaw, first infralabials connected with mental, second infralabial, inner and outer postmentals; inner pair of postmentals are larger than the outer postmentals, posterior margin of the inner postmentals bordered by eight granular scales of different size; one or two rows of enlarged scales along the infralabials starting below the outer postmentals, posteriorly size of those decreases, elongated and narrow; rest of the gular scales are small, granular juxtaposed, homogeneous, size increases towards throat where they become imbricate.

Habitus slender (BW/SVL = 0.18, TRL/SVL = 0.45), dorsoventrally depressed; dorsal scales granular, rounded, heterogeneous, intermixed with rounded, weakly keeled and bluntly conical tubercles irregularly arranged, starting from occipital region to fourth segment of the tail, size increases towards posterior body, pronounced at sacrum and base of the tail; 15 dorsal tubercles across mid dorsum; 26 paravertebral tubercles; ventrolateral fold weak; ventral scales larger than those of dorsal, flat, smooth, cycloid subimbricate to imbricate, largest on belly; 40 mid-ventral scales between ventrolateral fold; very small, 10 precloacal pores arranged in an inverted "V" shaped continuous series, followed by 7 unpored, large scales below it, largest at the apex.

Forelimbs and hindlimbs slender (FL/SVL = 0.14, CL/SVL = 0.17); digits strongly inflected at the joints, all bearing large recurved claw, enlarged subdigital lamellae, lamellae beneath digit IV of right and left manus (given as basal + distal) is 6+11 and 6+10 respectively, the second most lower lamellae of the basal series of digit IV of both sides are divided (not included in lamellar count); lamellae beneath digit IV of right and left pes (given as basal + distal) is 7+11 and 6+10 respectively; dorsal scales on forelimbs heterogeneous, granular juxtaposed, smooth and subimbricate at distal end of forearm; forearm intermixed with a few rounded, large tubercles; dorsal scales of hindlimbs granular intermixed with large, rounded, bluntly conical tubercles; scales on thigh towards knee smooth subimbricate; ventral scales of forelimbs granular, juxtaposed, mostly homogeneous; scales on palm heterogeneous, granular juxtaposed; scales on hindlimbs smaller than those of belly, smooth, cycloid and subimbricate; scales on the knee, above cloaca and on thigh below the level of precloacal pores are smaller and granular; scales on soles heterogeneous, granular, juxtaposed to subimbricate.

Tail complete, regenerated (TL = 80 mm), slender, gradually tapering, segments indistinct; dorsal scales

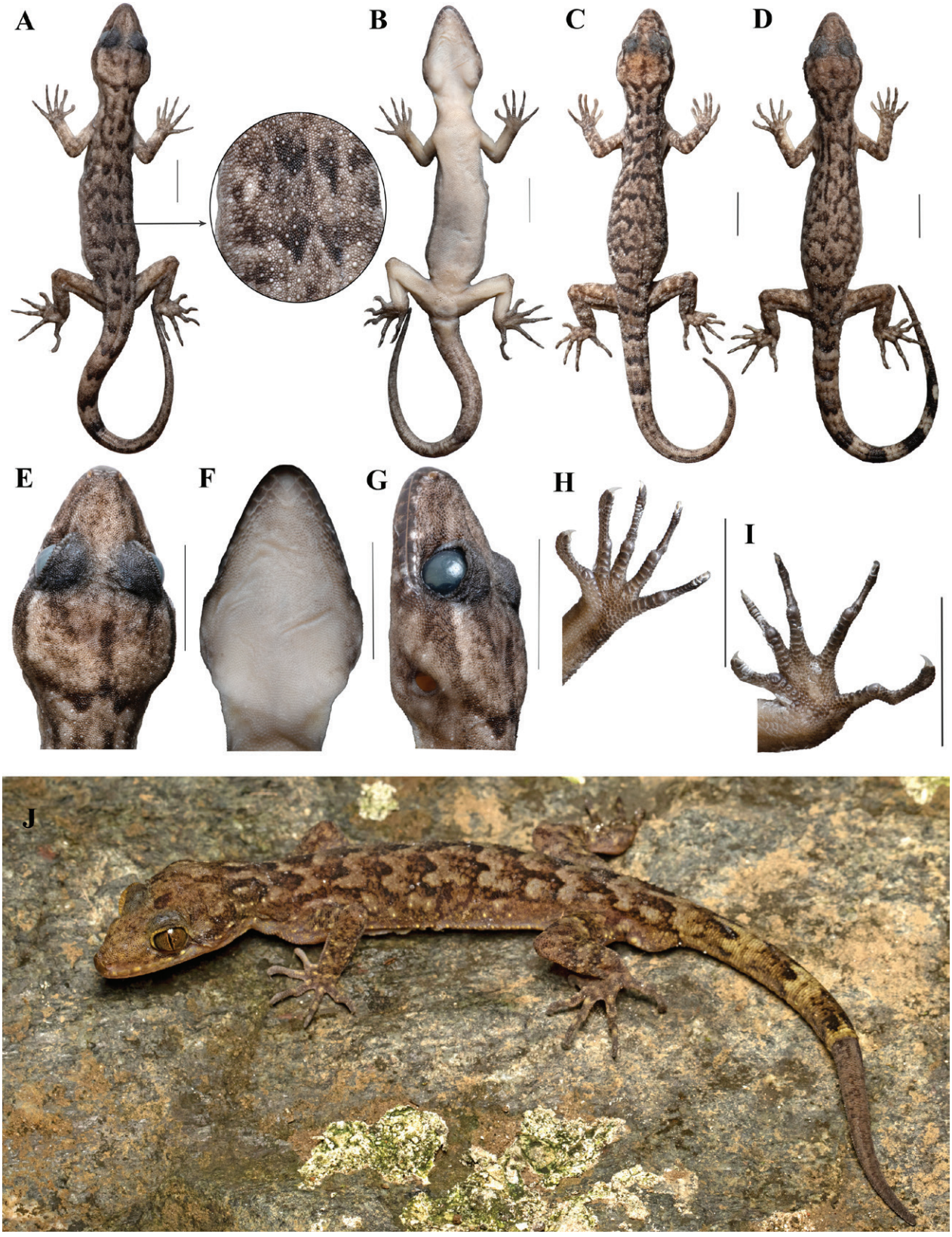

Figure 9. *Cyrtodactylus siangensis* **sp. nov. A**, **B**, **E**–**I** holotype (WII-ADR1177), **A** dorsal, and **B** ventral view of whole body; **C** paratype (WII-ADR1582); **D** paratype (WII-ADR1581); **E** dorsal, **F** ventral, and **G** lateral view of the head (WII-ADR1177); **H** ventral view of left manus, and **I** left pes (WII-ADR1177); **J** an uncollected male in natural habitat from Jorsing, East Siang, Arunachal Pradesh. Scale bar: 10 mm. **J** not to scale.

small, granular, juxtaposed at the base, posteriorly size increases, flat, smooth, subimbricate, heterogeneous in shape and size; large feebly keeled scales up to fourth segment of the tail at the distal end of each segment, those on basal segment are pronounced; subcaudal scales smooth, subimbricate, wider than that of dorsal, heteroge-

neous in shape and size; below cloaca scales are granular, smaller than the rest of the tail scales; no enlarged plate like series of subcaudal scales; three bluntly conical spurs on each side of the tail base present.

Colouration in preservative. Top of head, limbs and tail pale-brown; dorsum pale-greyish-brown; a slightly dark-brown stripe radiating from posterior orbital border to occipital region, medially "W" shaped; an another short dark-brown stripe at the middle of the head; a short, posteriorly diffused dark-brown stripe starting from posterior corner of the upper eyelids; a faint brown stripe on the loreal region; rostral and mental scale, labial scales dark-greyish-brown with white patch posteriorly; short and irregular shaped, longitudinal dark-brown stripe on dorsal side of neck; six irregular shaped, zig-zagged dark-brown bands on dorsum; irregular shaped, large dark-brown spots on sacrum and tail base; zig-zagged dark-brown bands on anterior part of the tail, posterior half of the tail (regenerated part) with brown speculation; indistinct brown reticulation on dorsal side of the limbs; ventrally head, body and limbs creamy-white with brown speculation; chin scales and scales below infralabials heavily speckled; lamellae, palm and feet heavily speckled with brown; indistinct brown patches on ventral side of the tail.

Morphological variation. Detailed morphological variations among the collected individuals of *Cyrtodactylus siangensis* are provided in Table S2. Dorsal dark brown markings in the two paratypes are variable in the form of irregular zig-zagged bands to reticulation; reticulation on limbs of the two paratypes distinct than the holotype; cross bands on tail of WII-ADR1581 darker posteriorly (Fig. 9).

Comparison. Morphologically *Cyrtodactylus siangensis* **sp. nov.** is close to *C. cayuensis*, however, phylogenetically it is distinct from the later (Fig. 2; Table S3), also the type locality of the new species is separated by Siang River from the *C. cayuensis* localities recorded in this study (Fig. 3B). Morphological differences with other members of *khasiensis* group is presented in Table 2.

Sequence divergence. *Cyrtodactylus siangensis* **sp. nov.** has a high genetic divergence of 11.7–17.0% from its closely related and the only other species in the clade, *C. cayuensis*.

Etymology. The specific epithet is a toponym derived from the name of the river "Siang". The type locality of this species lies in the Siang valley of Arunachal Pradesh.

Suggested common name. Siang Valley bent-toed gecko.

Distribution and natural history. *Cyrtodactylus siangensis* **sp. nov.** is currently only known from the type locality, Bodak, East Siang District. It appears to be uncommon, and likely a habitat generalist. The holotype was encountered on a shrub at the edge of Kalek stream (a tributary of Siang River) at a height of approximately one meter above the ground, at 18:15 hrs. The stream at the time of survey was flowing at a moderately speed, was approximately 10 m in width and contained boulders (sedimentary rock) and fallen logs. The two paratypes were recorded on a small tree at a height of 2.0 m on the slope of a hill close to the collection site for the holotype. The type locality is ca. 300 m from Siang River and approximately 150 m from the road connecting Pasighat and Yinkiong.

Expanded description of *Cyrtodactylus cayuensis* Li, 2007

Figures 10, S3; Tables 2, S4

Chresonyms.
Cyrtodactylus khasiensis cayuensis – Li (2007)
Cyrtodactylus cayuensis – Agarwal et al. (2018: 337)
Cyrtodactylus arunachalensis – Mirza et al. (2021)

Materials examined. (Fig. 10). Arunachal Pradesh: one male (WII-ADR1219) and one female (WII-ADR1218) collected from Balek village (28.0624°N; 95.2721°E; elevation 450 m a.s.l.), East Siang District on 29 October 2021 by Bitupan Boruah; one male (WII-ADR1213) collected from Ramsing (28.6563°N; 94.9795°E; elevation 600 m a.s.l.), Mouling National Park, Upper Siang District on 27 October 2021 by Bitupan Boruah; one female (WII-ADR1199) collected from Syrnyup stream (28.5340°N; 95.0305°E; elevation 890 m a.s.l.), Jengging, Mouling National Park, Upper Siang District on 26 October 2021 by Bitupan Boruah; two males (WII-ADR695 and WII-ADR696) and two females (WII-ADR697 and WII-ADR698) collected from Potin (27.3478°N, 93.8497°E, elevation 900 m a.s.l.), Lower Subansiri District on 5 October 2019 by Bitupan Boruah; one female (WII-ADR3017) collected near Glaw lake (27.6960°N; 96.4456°E; elevation 1200 m a.s.l.), Kamlang Tiger Reserve, Lohit District on 2 September 2022 by Abhijit Das, Bitupan Boruah and Naitik G. Patel; one male (WII-ADR1682) and one female (WII-ADR1681) collected from Ezengo (28.1565°N; 95.8638°E; elevation 560 m a.s.l.), Lower Dibang Valley District on 3 August 2022 By Bitupan Boruah; three females (WII-ADR453, WII-ADR454 and WII-ADR459) collected from Jengging (28.5499°N; 95.0537°E; elevation 760 m a.s.l.) by Abhijit Das on 5 October 2018; one female (WII-ADR478) and one male (WII-ADR473) collected from 6 km northwest to Pasighat (28.0945°N; 95.2682°E; elevation 410 m a.s.l.) by Abhijit Das on 2 October 2018.

Revised diagnosis. Medium-sized gecko, SVL 61.2–83.5 mm in adult males and SVL 59.4–83.6 mm in adult females; 8–13 supralabials and 8–12 infralabials; 18–26 rows of bluntly conical and feebly keeled enlarged tubercles across mid-dorsum; 27–38 paravertebral tubercles between the level of axilla and groin; 28–44 mid-ventral scales; 13–21 subdigital lamellae beneath the fourth digit

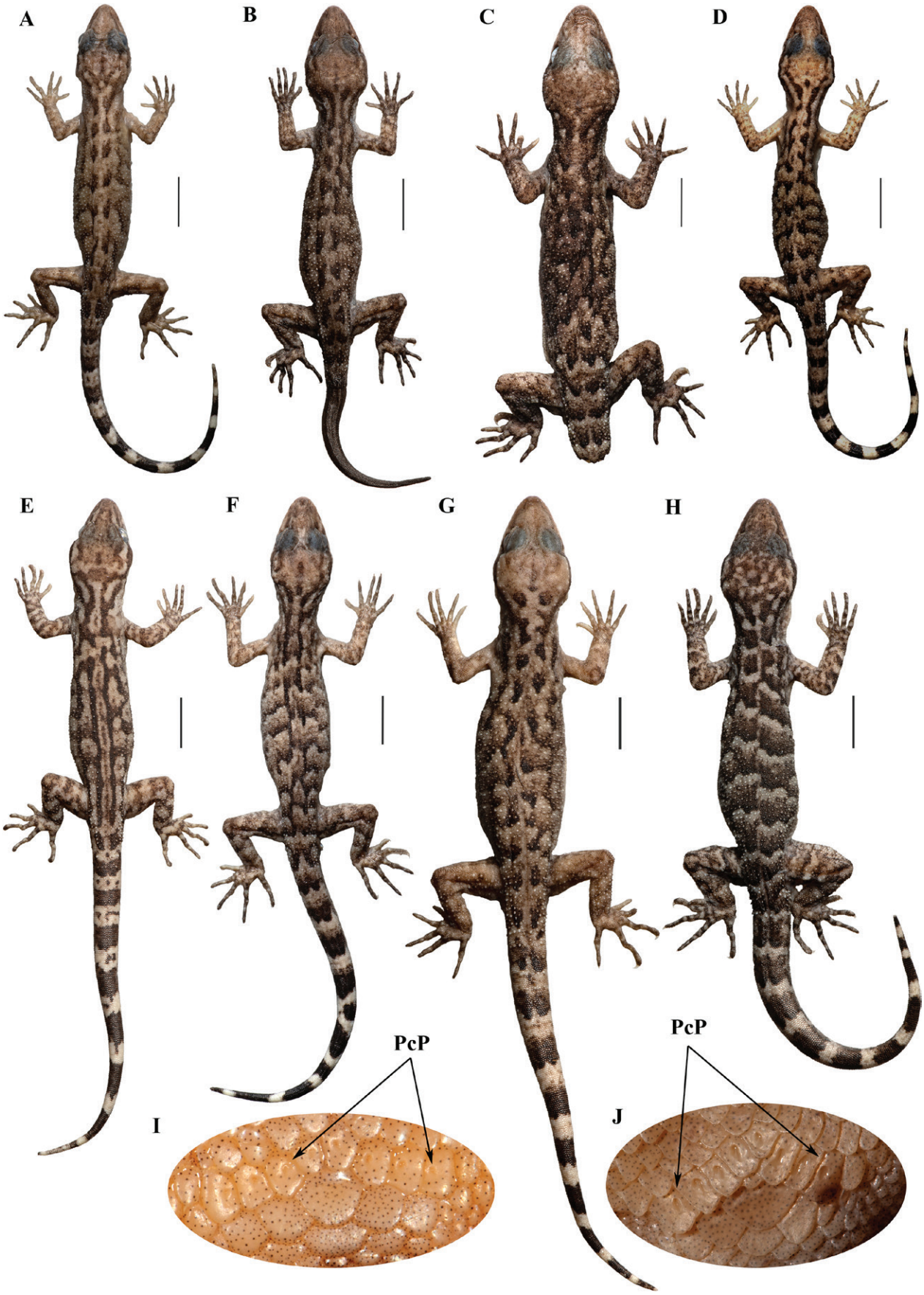

Figure 10. *Cyrtodactylus cayuensis* from India showing the variation in dorsal marking pattern. **A** WII-ADR1219 (Balek), **B** WII-ADR1681 (Ezengo), **C** WII-ADR1199 (Jengging), **D** WII-ADR1218 (Balek), **E** WII-ADR454 (Jengging), **F** WII-ADR1213 (Ramsing), **G** WII-ADR698 (Potin), **H** WII-ADR3017 (Glaw lake), **I** precloacal pores in WII-ADR698, and **J** precloacal pores in WII-ADR478. Scale bar: 10 mm. **I**, **J** not to scale.

of manus; 11–23 subdigital lamellae beneath the fourth digit of pes; colouration and marking pattern variable; dorsally greyish-brown, pale-brown or pale-yellowish-brown; five to eight dark-brown bands consisting of irregular shaped and sized enlarged spots on back between axilla and groin, or dorsum with dark-brown reticulation; tail with 9–13 dark and 9–12 light bands alternatively arranged on top.

Description based on newly collected materials. Medium-sized gecko, SVL 61.2–75.1 mm in males (n = 6) and SVL 59.4–83.6 mm in females (n = 11); head moderately large (HL/SVL = 0.25–0.28), dorsoventrally depressed, longer than width (HW/HL = 0.67–0.75), distinct from neck, broader at occipital region; snout rounded in both dorsal and lateral view; loreal region convex; canthus rostralis rounded, indistinct; interorbital space flat, a longitudinal furrow on dorsal surface of the snout, snout short (SO/HL = 0.38–0.43), longer than orbit (OD/SO = 0.49–0.78); nostril opening directed posterolaterally; ear opening oblique; scales on head heterogeneous, largest on snout and loreal region, posteriorly smaller in upper eyelid, interorbital space and occipital region, granular juxtaposed; scales on upper eyelids heterogeneous; supraciliaries outwardly sharp giving serrated appearance in dorsal view, size anteriorly and posteriorly decreases; rostral wide, a short groove at the middle on top; granular scales at parietal region and occipital region intermixed with slightly large rounded granular tubercles, dense in occipital and temporal region and size increases towards nape; 9–13 supralabials present, size decreases towards angle of jaw; a series of scales, slightly larger than the loreal scales present above the supralabials; 8–12 infralabials, size decreases towards angle of jaw; two or three rows of slightly enlarged and narrow scales along the infralabials, posteriorly size of those decreases; rest of the gular scales are small, granular juxtaposed, nearly homogeneous, scales on throat are imbricate.

Habitus slender (BW/SVL = 0.16–0.22, TRL/SVL = 0.41–0.47), dorsoventrally depressed; dorsal scales granular, heterogeneous, intermixed with rounded, weakly keeled and bluntly conical tubercles irregularly arranged, continuing up to third or fifth segment of the tail, size of the tubercles increases towards posterior body, pronounced at sacrum and base of the tail, posteriormost rows indistinctly keeled; 15–21 rows of dorsal tubercles across mid dorsum; 27–38 paravertebral tubercles; ventrolateral fold present; ventral scales on chest and belly larger than those of dorsal, flat, smooth, cycloid, subimbricate to imbricate; 34–44 mid ventral scales; seven or nine distinct precloacal pores in male and 7–10 small precloacal pores in female; PcP followed by three to six unpored enlarged scales below.

Forelimbs and hindlimbs slender (FL/SVL = 0.13–0.15, CL/SVL = 0.16–0.18); digits strongly inflected at the joints, all bearing large recurved claw and enlarged subdigital lamellae, dorsal scales on forelimbs heterogeneous, granular juxtaposed, smooth and subimbricate at distal end of forearm; forearm intermixed with a few rounded, large tubercles; dorsal scales of hindlimbs granular intermixed with large, rounded, bluntly conical tubercles; thigh scales towards lateral and dorsolateral side are smooth and subimbricate; ventral scales of forelimbs granular, juxtaposed, mostly homogeneous; scales on palm heterogeneous, granular juxtaposed; scales on ventral side of hindlimbs slightly smaller than or nearly equal to those of belly, smooth, cycloid and subimbricate; scales on the knee, above cloaca and on thigh below the level of precloacal pores are smaller and granular; scales on soles heterogeneous, granular, juxtaposed to subimbricate.

Tail slender (TL = 58–97 mm), gradually tapering, segments indistinct; dorsal scales small, granular, juxtaposed at the base, posteriorly size increases, flat, smooth, subimbricate, heterogeneous in shape and size; large feebly keeled scales up to third to fifth segment of the tail, those on basal segment are pronounced and posterior rows with indistinct keel; subcaudal scales smooth, subimbricate, wider than that of dorsal, heterogeneous in shape and size; no enlarged plate like series of subcaudal scales; two to four bluntly conical spurs present at the base of the tail. Detailed morphological characteristics of the collected samples are provided in Table S4.

Sequence divergence. The intraspecific divergence within *C. cayuensis* ranges between 0.1–6.4%. Among the two clades identified by bPTP, both clades have an intraspecific divergence between 0.1–4.3% and 0.2–2.4%, respectively. The divergence between these two clades range between 3–6.4%.

Colouration in life. Dorsal colour and marking pattern variable (Fig. S3). Head and body greyish-brown, pale-brown to pale-yellowish-brown on top; head on top irregularly mottled with dark-brown, slightly enlarged dark-brown irregular patches may be present on occipital area; dark-brown postorbital stripe and loreal stripe present; a light stripe above loreal stripe and postorbital stripe may be visible; a few pale-yellow spots may be present on temporal and occipital region; supraciliary yellowish-brown; neck with short dark-brown streak with irregular edge or with irregular shaped patches; trunk dorsally with five to eight dark-brown bands consisting of irregular shaped and sized enlarged spots and posteriorly pale-yellowish or light-edged, these bands mid dorsally interrupted, or dorsum with dark-brown reticulation; limbs dorsally greyish-brown or pale-yellowish-brown or pale-brown with distinct or indistinct dark-brown reticulation; a dark-brown band on sacrum, band mid dorsally intersected; tail dorsally with 9–13 dark and 9–12 light bands alternatively arranged, bands are with irregular edged, anterior one or two dark bands may be mid dorsally intersected, dark bands are broad and light bands are comparatively narrow, dark bands are posteriorly becomes black or more dark-brown, while light bands become whitish; light bands may have a few dark-brown spots.

Distribution and natural history. The type locality, Xizang (Tibet), China by *C. cayuensis* also appears to be widely distributed in Arunachal Pradesh, India

(Fig. 3B), within an elevational range of 410–1200 m a.s.l. *Cyrtodactylus cayuensis* is widespread in the foothills of Arunachal Pradesh from the western part of the state, at Seijusa (Pakke Tiger Reserve) to the eastern part (Kamlang Tiger Reserve) and it has successfully spread across major tributaries of the Brahmaputra River, i.e., the Subansiri, Siang, Dibang, Lohit up to at least north of Noa-Dihing. Populations of *C. cayuensis* have been recorded in degraded evergreen forest as well as in undisturbed semi-evergreen and evergreen forests. *Cyrtodactylus cayuensis* is particularly abundant in the vegetation close to the picturesque Glaw Lake in the Kamlang Tiger Reserve. We observed individuals at night on shrubs and bedrocks (sedimentary rock) along small forest streams. We also encountered them on small trees up to a 2.0 m inside the forest at Jengging, Kamlang Tiger Reserve and Mehao Wildlife Sanctuary.

Discussion

The description of six new species of *Cyrtodactylus* from northeastern India demonstrates the hidden diversity and reiterates the need for further exploration of this region. With the addition of these new species, *Cyrtodactylus* now comprises 364 species out of which 10% (35 species) are in the *khasiensis* group. Earlier, Agarwal et al. (2014) defined the *khasiensis* clade as a clade distributed south of Brahmaputra River, but Mirza et al. (2021)'s samples from the north of this river fell within this clade and showed the presence of what they thought was a distinct lineage (*C. arunachalensis* **syn. nov.**) north of the Brahmaputra River. Based on the current findings, we now report another species, *C. siangensis* **sp. nov.** from north of Brahmaputra River.

Our decision on the status of *C. arunachalensis*, and considering that clade as a single species *C. cayuensis* is conservative at this time. All the samples from this clade (excluding the new species, *Cyrtodactylus siangensis* **sp. nov.**) are from the low to mid elevations and the minor genetic variations within the clade could be due to the presence of river barriers and/or sampling gaps. Additionally, some low elevation species are known to be widespread compared to their more montane congeners (Grismer et al. 2012, 2014; Vogel et al. 2022). Conversely, several recently described species within the *khasiensis* group and other gekkonid genera were based on a 3–5% threshold in the ND2 sequence divergence (Agarwal et al. 2018a, 2018b; Chomdej et al. 2023). Although the clade from the East Siang (Balek, Jenging and Ramsing), is 3–6.3% distinct from the other samples of *C. cayuensis*, describing it as a distinct species would result in a disjunct distribution of *C. cayuensis* (Table S3). Therefore, due to sampling gaps observed in other lower elevation species in Arunachal Pradesh, we refrain from splitting this clade into multiple species at this time. Furthermore, after examining specimens and comparing them with *C. cayuensis* there were no diagnostic morphological characters that separated the subclades in the lower elevations. Additional and a much denser sampling in the regions north of Brahmaputra River will help in our better understanding of the relationships between the lower elevation populations.

Out of the six new species described here, *C. barailensis* **sp. nov.** and *C. manipurensis* **sp. nov.** are based on single specimens. In the morphological context, *C. barailensis* **sp. nov.** differs from its sister *C. namtiram* in having fewer dorsal tubercle rows (DTR 17 vs. DTR 21), dorsal marking pattern (dark-brown reticulation on dorsum vs. seven pairs of dark-brown blotches on the dorsum) and they are geographically separated from each other by 58 km (aerial distance), and *C. manipurensis* **sp. nov.** by fewer dorsal tubercle rows, DTR 17 and paravertebral tubercles, PVT 32 (vs. DTR 21 and PVT 37) (Table 2). It is also pertinent to add that several other *Cyrtodactylus* species in the recent past were described based on single specimens, that are genetically distinct (Agarwal et al. 2018b; Grismer et al. 2018; Mahony and Kamei 2021; Chomdej et al. 2023). Despite these two species being genetically distinct, we do acknowledge that their morphological diagnoses may be incomplete. Additional sampling may show that some of these characters are not diagnostic just as additional sampling may indicate that others are. This has no bearing on the delimitation of these species in the phylogeny.

The genus *Cyrtodactylus* has its southwestern-most distribution in Sri Lanka and eastern-most distribution in the Solomon Islands (Grismer et al. 2021) showing their ability to radiate across biogeographic barriers. In the Himalayan region (including Bhutan, Nepal, and Pakistan) and northeast India, there are a total of 39 species but there is stark contrast in the number of species in these two regions. The Himalayas are depauperate (nine species) compared to northeast India (28 species) (Agarwal et al. 2014; Schleich and Kästle 2002). This pattern could be due to various factors including rainfall, temperature, seasonality, and vegetation type (Fig. 11). Furthermore, the Eastern Himalayas exhibit faunal exchanges with Indo-Burma and the Western Himalaya and the distribution of *Cyrtodactylus* terminates in the Western Himalayas. Among the four clades of *khasiensis* group found in northeastern India, the *gansi* clade is most diverse with 13 species entirely distributed south of Brahmaputra River. The *khasiensis* clade contains 11 species in the region and except for *C. septentrionalis*, all the members are also distributed south of Brahmaputra River. While the *cayuensis* clade now contains two species, from which *C. cayuensis* is widely distributed along the Himalayan foothills north of Brahmaputra River and eastern part of the region in Dibang valley. The *mombergi* clade has one Indian species, which we described here is distributed in the eastern part of the region along Noa-Dihing River and Lohit River valley (Fig. 3). Most species found in the Northeast Hill region appear to be endemic and highly cryptic. Identification of such hidden diversity appears to be crucial for setting conservation values of biodiversity hotspots which are threatened by rapid deforestation.

Figure 11. Habitats of newly described species of *Cyrtodactylus* from northeastern India. **A** landscape view of Kiphire near the type locality of *C. kiphire* **sp. nov.**; **B** forest cover of Barail hills near type locality of *C. barailensis* **sp. nov.**; **C** view of hills at Namdapha Tiger Reserve and **D** forest trail at Kamala Valley, type locality of *C. namdaphaensis* **sp. nov.**; **E** low land forest stream at Ngengpui Wildlife Sanctuary, type locality of *C. ngengpuiensis* **sp. nov.**, **F** landscape view of Saing River and Adi hills at the type locality of *C. siangensis* **sp. nov.**

Acknowledgements

We thank the National Geographic Society for the award of National Geographic Explorer Grant (NGS-74044R-20) and SERB-DST (CRG/2018/000790) for financial support. Fieldwork is possible due to permission and logistics by the state forest departments of Arunachal Pradesh, Meghalaya, Mizoram, Manipur and Nagaland (vide letter nos. CWL/GEN/13(95)/11-12/Pt.V/438-40 dated 2 May 2018; CWL/G/173/2018-19/Pt.VII/1100-07 dated 22 August 2019; CWL/GEN/96(Vol-III)/550 dated 8 July, 2019; B.19060/1/2020-CWLW/112 dated 2 February 2021; CWL/GEN/355/2021/3178 dated 28 September 2021; FOR.77/2019/66 dated 27 June, 2022; CWL/173/2018-19/Prt. VII(A)/296-303 dated 20 April 2023). We sincerely acknowledge the support received from officials of Arunachal Pradesh Forest Department namely Sh. Milo Taser, Sh. Aduk Paron, Sh. Tajum Yomcha, Sh. Dhawan Kumar Rawat, Sh. Harshraj Wathore, Sh. Bunty Tao, Sh. B. Darang, Sh. Kabuk Lego, Sh. Taluk Rime, Sh. Rupir Boli, Sh. Kamin Dai, Sh. Tashi Mize, Sh. Mayur Variya, Sh. Aditya Das for their support during field work. We thank Sh. Aochuba (Field director, Intanki NP, Nagaland), Bendang Temsu (Range Officer, Kiphire, Nagaland), Limthure Yimchunger (Nagaland). We thank B. Lalrinmuanpuia (Mizoram) and Parsanga (Ngengpui) for their help. Our sincere thanks to Sh. Arpiyush Sangma (Meghalaya Forest dept.) for valuable support. We thank Sh. Virendra R. Twari (Director), Ruchi Badola (Dean) and Sh. S. Sathya-

kumar (Registrar) of Wildlife Institute of India, Dehradun for their constant support. We thank Rajiv N.V., Jason D. Gerard, Vijayan Jithin, Santanu Dey, Sourav Dutta, Naitik G. Patel, Krishnendu Banerjee, Pranoy K. Borah, Vignesh, Mirza G. Ghazi, Neelam Dutta, Malsawmdawngliana, Isaac Zosangliana, K. Lalhmangaiha, Deb Sankha Goswami and Swati Nawani for their help during field work. We thank Mark O'Shea, University of Wolverhampton, UK for language corrections in an earlier draft of this manuscript. We thank field assistants Lishi Gunia, Aphu Yoha Yobin, Akhida and John Tayeng and Brinton Warjri. We are thankful to and we miss Late Teibor Marwein who helped a lot during our field work in Meghalaya. We thank A. Madhanraj, Surya Prasad Sharma, and Kumudani Bala Gautam for their help during lab work. We thank S.K. Dutta and Indraneil Das, Samrat Mondol for their support. VD thanks Uwe Fritz at the Senckenberg Dresden and Simon Maddock at Newcastle University for their support. SN and NAA's contributions are supported by National Geographic Society for the award of National Geographic Explorer Grant (NGS-71945C-20), Global Conservation Foundation. SN and NAA thank FELIS Creations and team for the support during the fieldwork in Siang Valley, Arunachal Pradesh, India. SN also thanks Soubadra Devy, ATREE, Bengaluru and the team for the valuable support in the field. We thank L. Lee Grismer, Pratyush P. Mohapatra and the anonymous reviewer for their comments, which improved this manuscript.

References

Agarwal I, Bauer AM, Jackman TR, Karanth KP (2014) Insights into Himalayan biogeography from geckos: A molecular phylogeny of *Cyrtodactylus* (Squamata: Gekkonidae). Molecular Phylogenetics and Evolution 80: 145–155. https://doi.org/10.1016/j.ympev.2014.07.018

Agarwal I, Mahony S, Giri VB, Chaitanya R, Bauer AM (2018a) Two new species of *Cyrtodactylus* Gray, 1827 (Squamata: Gekkonidae) with comments on name-bearing types from northeast India. Zootaxa 4420: 334–356. https://doi.org/10.11646/zootaxa.4420.3

Agarwal I, Mahony S, Giri VB, Chaitanya R, Bauer AM (2018b) Six new *Cyrtodactylus* (Squamata: Gekkonidae) from northeast India. Zootaxa 4524: 501–535. https://doi.org/10.11646/zootaxa.4524.5.1

Bauer AM (2002) Two new species of *Cyrtodactylus* (Squamata: Gekkonidae) from Myanmar. Proceedings of the California Academy of Sciences 53: 73–86.

Bauer AM (2003) Descriptions of seven new *Cyrtodactylus* (Squamata: Gekkonidae) with a key to the species of Myanmar (Burma). Proceedings of the California Academy of Sciences 54: 463–498.

Bohra SC, Zonunsanga HT, Das M, Purkayastha J, Biakzuala L, Lalremsanga HT (2022) Morphological and molecular phylogenetic data reveal another new species of bent-toed gecko (*Cyrtodactylus* Gray: Squamata: Gekkonidae) from Mizoram, India. Journal of Natural History 56: 1585–608. https://doi.org/10.1080/00222933.2022.2119178

Che J, Jiang K, Yan F, Zhang Y-P (2020) Amphibians and Reptiles in Tibet—Diversity and Evolution. Chinese Academy of Sciences. Science Press, Beijing [in Chinese].

Chomdej S, Suwannapoom C, Pradit W, Phupanbai A, Grismer LL (2023) A new species of the *Cyrtodactylus brevipalmatus* group (Squamata, Gekkonidae) from Tak Province, northwestern Thailand. ZooKeys 1164: 63–88. https://doi.org/10.3897/zookeys.1164.101263

Das S, Pal S, Siddharth S, Palot MJ, Deepak V, Narayanan S (2022) A new species of large-bodied *Hemidactylus* Goldfuss, 1820 (Squamata: Gekkonidae) from the Western Ghats of India. Vertebrate Zoology 72: 81–94. https://doi.org/10.3897/vz.72.e76046

Grismer LL, Wood Jr PL, Quah ES, Anuar S, Muin MA, Sumontha M, Ahmad N, Bauer AM, Wangkulangkul S, Grismer JL, Pauwels OS (2012) A phylogeny and taxonomy of the Thai-Malay Peninsula Bent-toed Geckos of the *Cyrtodactylus pulchellus* complex (Squamata: Gekkonidae): Combined morphological and molecular analyses with descriptions of seven new species. Zootaxa 3520: 1–55. https://doi.org/10.11646/zootaxa.3520.1.1

Grismer LL, Wood Jr PL, Anuar S, Quah ES, Muin MA, Mohamed M, Chan KO, Sumarli AX, Loredo AI, Heinz HM (2014) The phylogenetic relationships of three new species of the *Cyrtodactylus pulchellus* complex (Squamata: Gekkonidae) from poorly explored regions in northeastern Peninsular Malaysia. Zootaxa 3786: 359–381. https://doi.org/10.11646/zootaxa.3786.3.6

Grismer LL, Wood Jr PL, Thura MK, Win NM, Grismer MS, Trueblood LA, Quah ESH (2018) A redescription of *Cyrtodactylus chrysopylos* Bauer (Squamata: Gekkonidae) with comments on the adaptive significance of orange coloration in hatchlings and descriptions of two new species from eastern Myanmar (Burma). Zootaxa 4527: 151–185. https://doi.org/10.11646/zootaxa.4527.2.1

Grismer LL, Wood Jr PL, Quah ESH, Thura MK, Herr MW, Lin AK (2019) A new species of forest-dwelling *Cyrtodactylus* Gray (Squamata: Gekkonidae) from the Indawgyi Wildlife Sanctuary, Kachin State, Myanmar. Zootaxa 4623: 1–25. https://doi.org/10.11646/zootaxa.4623.1.1

Grismer LL, Wood Jr PL, Poyarkov NA, Le MD, Kraus F, Agarwal I, Oliver PM, Nguyen SN, Nguyen TQ, Karunarathna S, Welton LJ, Stuart BL, Luu VQ, Bauer AM, O'Connell KA, Quah ESH, Chan KO, Ziegler T, Ngo H, Nazarov RA, Aowphol A, Chomdej S, Suwannapoom C, Siler CD, Anuar S, Tri NV, Grismer JL (2021) Phylogenetic partitioning of the third-largest vertebrate genus in the world, *Cyrtodactylus* Gray, 1827 (Reptilia; Squamata; Gekkonidae) and its relevance to taxonomy and conservation. Vertebrate Zoology 71: 101–154. https://doi.org/10.3897/vz.71.e59307

Grismer LL, Poyarkov NA, Quah ESH, Grismer JL, Wood Jr PL (2022) The biogeography of bent-toed geckos, *Cyrtodactylus* (Squamata: Gekkonidae). PeerJ 10: e13153 http://doi.org/10.7717/peerj.13153

Kamei RG, Mahony S (2021) A new species of Bent-toed gecko (Squamata: Gekkonidae: *Cyrtodactylus* Gray, 1827) from the Garo Hills, Meghalaya State, north-east India, and discussion of morphological variation for *C. urbanus*. Herpetological Journal 31: 177–196. https://doi.org/10.33256/31.3.177196

Kalyaanamoorthy S, Minh BQ, Wong TK, Von Haeseler A, Jermiin LS (2017) ModelFinder: Fast model selection for accurate phylogenetic estimates. Nature Methods 14: 587–589. https://doi.org/10.1038/nmeth.4285

Kumar S, Stecher G, Tamura K (2016) MEGA7: Molecular Evolutionary Genetics Analysis version 7.0 for bigger datasets. Molecular Biology and Evolution 33: 1870–1874. https://doi.org/10.1093/molbev/msw054

Lalremsanga HT, Chinliansiama H, Bohra SC, Biakzuala L, Vabeiryureilai M, Muansanga L, Malsawmdawngliana F, Hmar GZ, Decemson H, Siammawii V, Das M (2022) A new bent-toed gecko (*Cyrtodactylus* Gray: Squamata: Gekkonidae) from the state of Mizoram, India. Zootaxa 5093: 465–482. https://doi.org/10.11646/zootaxa.5093.4.5

Lalremsanga HT, Colney Z, Vabeiryureilai M, Malsawmdawngliana F, Bohra SC, Biakzuala L, Muansanga L, Das M, Purkayastha J (2023) It's all in the name: Another new *Cyrtodactylus* Gray (Squamata:

Gekkonidae) from northern Mizoram, North-east India. Zootaxa 5369: 553–575. https://doi.org/10.11646/zootaxa.5369.4.5

Lanfear R, Frandsen PB, Wright AM, Senfeld T, Calcott B (2017) PartitionFinder 2: New Methods for Selecting Partitioned Models of Evolution for Molecular and Morphological Phylogenetic Analyses. Molecular Biology and Evolution 34: 772–773. https://doi.org/10.1093/molbev/msw260

Li PP (2007) Description of a new subspecies of *Cyrtodactylus khasiensis* from China. Acta Zootaxonomica Sinica 32: 733–737.

Liu S, Rao D (2022) A new species of *Cyrtodactylus* Gray, 1827 (Squamata, Gekkonidae) from south-western Yunnan, China. ZooKeys 1084: 83–100. https://doi.org/10.3897/zookeys.1084.72868

Macey JR, Larson A, Ananjeva NB, Fang Z, Papenfuss TJ (1997) Two novel gene orders and the role of light-strand replication in rearrangement of the vertebrate mitochondrial genome. Molecular Biology and Evolution 14: 91–104. https://doi.org/10.1093/oxfordjournals.molbev.a025706

Mahony S (2009) Taxonomic status of *Cyrtodactylus khasiensis tamaiensis* (Smith, 1940) and description of a new species allied to *C. chrysopylos* Bauer, 2003 from Myanmar (Reptilia: Gekkonidae). Hamadryad 34: 62–74.

Mahony S, Kamei RG (2021) A new species of *Cyrtodactylus* Gray (Squamata: Gekkonidae) from Manipur State, northeast India, with a critical review highlighting extensive errors in literature covering bent-toed geckos of the Indo-Burma region. Journal of Natural History 55: 2445–2480. https://doi.org/10.1080/00222933.2021.1994667

Minh BQ, Nguyen MAT, von Haeseler, A (2013) Ultrafast approximation for phylogenetic bootstrap. Molecular Biology and Evolution 30: 1188–1195. https://doi.org/10.1093/molbev/mst024

Mirza ZA, Bhosale H, Ansari F, Phansalkar P, Sawant M, Gowande G, Patel H (2021) A new species of geckos of the genus *Cyrtodactylus* Gray, 1827 from Arunachal Pradesh, India. Evolutionary Systematics 5: 13–23. https://doi.org/10.3897/evolsyst.5.61667

Mirza ZA, Bhosale HS, Thackeray T, Phansalkar P, Sawant M, Gowande GG, Patel H (2022) A new species of bent-toed geckos of the genus *Cyrtodactylus* Gray, 1827 from western Arunachal Pradesh, India. Herpetozoa 35: 65–76. https://doi.org/10.3897/herpetozoa.35.e80610

Purkayastha J, Das M, Bohra SC, Bauer AM, Agarwal I (2020) Another new *Cyrtodactylus* (Squamata: Gekkonidae) from Guwahati, Assam, India. Zootaxa 4732: 375–392. https://doi.org/10.11646/zootaxa.4732.3.2

Purkayastha J, Lalremsanga HT, Bohra SC, Biakzuala L, Decemson H, Muansanga L, Vabeiryureilai M, Chauhan S, Rathee YS (2021) Four new bent-toed geckos (*Cyrtodactylus* Gray: Squamata: Gekkonidae) from northeast India. Zootaxa 4980: 451–489. https://doi.org/10.11646/zootaxa.4980.3.2

Purkayastha J, Lalremsanga HT, Litho B, Rathee YS, Bohra SC, Vabeiryureilai M, Biakzuala, L, Muansanga L (2022) Two new *Cyrtodactylus* (Squamata, Gekkonidae) from Northeast India. European Journal of Taxonomy 794: 111–139. https://doi.org/10.5852/ejt.2022.794.1659

Ronquist F, Teslenko M, Mark VDP, Ayres D, Darling A, Höhna S, Larget B, Liu L, Suchard MA, Huelsenbeck JP (2012) MrBayes 3.2: Efficient Bayesian phylogenetic inference and model choice across a large model space. Systematic Biology 61: 539–542. https://doi.org/10.1093/sysbio/sys029

Schleich HH, Kästle W (2002) Amphibians and Reptiles of Nepal. Biology, Systematics, Field Guide. Koeltz Scientific Books, Koenigstein, Germany.

Thompson JD, Higgins DG, Gibson TJ (1994) CLUSTAL W: Improving the sensitivity of progressive multiple sequence alignment through sequence weighting, position-specific gap penalties and weight matrix choice. Nucleic Acids Research 22: 4673–4680. https://doi.org/10.1093/nar/22.22.4673

Trifinopoulos J, Nguyen LT, von Haeseler A, Minh BQ (2016) Nucleic Acids Research 44: W232–W235. https://doi.org/10.1093/nar/gkw256

Wood Jr PL, Heinicke MP, Jackman TR, Bauer AM (2012) Phylogeny of bent-toed geckos (*Cyrtodactylus*) reveals a west to east pattern of diversification. Molecular Phylogenetics and Evolution 65: 992–1003. https://doi.org/10.1016/j.ympev.2012.08.025

Vences M, Miralles A, Brouillet S, Ducasse J, Fedosov A, Kharchev V, Kumari S, Patmanidis S, Puillandre N, Scherz MD, Kostadinov I, Renner SS (2021) iTaxoTools 0.1: Kickstarting a specimen-based software toolkit for taxonomists. Megataxa 6: 77–92. https://doi.org/10.11646/megataxa.6.2.1

Vogel G, Mallik AK, Chandramouli SR, Sharma V, Ganesh SR (2022) A review of records of the *Trimeresurus albolabris* Gray, 1842 group from the Indian subcontinent: Expanded description and range extension of *Trimeresurus salazar*, redescription of *Trimeresurus septentrionalis* and rediscovery of historical specimens of *Trimeresurus davidi* (Reptilia: Viperidae). Zootaxa 5175: 343–366. https://doi.org/10.11646/zootaxa.5175.3.2

Zhang D, Wu Y, Zuo C, Yin F, Liu S (2024) First description of the female of *Cyrtodactylus dianxiensis* Liu & Rao, 2021, with extended diagnosis of this species (Squamata, Gekkonidae). Herpetozoa 37: 65–72. https://doi.org/10.3897/herpetozoa.37.e119492

Supplementary Material 1

Figures S1–S3

Authors: Boruah B, Narayanan S, Aravind NA, Lalronunga S, Deepak V, Das A (2024)
Data type: .zip
Explanation notes: Figure S1. Phylogenetic relationship of *Cyrtodactylus* spp. of *khasiensis* group. — **Figure S2.** Morphological variation among the individuals of *C. namdaphaensis* **sp. nov.** — **Figure S3.** Variation of live coloration and pattern among the individuals of *C. cayuensis*.

Link: https://doi.org/10.3897/vz.74.e124752.suppl1

Supplementary Material 2

Tables S1–S4

Authors: Boruah B, Narayanan S, Aravind NA, Lalronunga S, Deepak V, Das A (2024)
Data type: .zip
Explanation notes: Table S1. GenBank voucher numbers and locality details for the DNA sequences used in this study. — **Table S2.** Morphological characters of the six newly described *Cyrtodactylus* species. — **Table S3.** P-Distance among the *Cyrtodactylus* spp. of *khaisensis* group. — **Table S4.** Morphological characters of *C. cayuensis* from Arunachal Pradesh collected in this study.

Link: https://doi.org/10.3897/vz.74.e124752.suppl2